

Review
Features of near-extremal
black holes

Geoffrey Compère
Université Libre de Bruxelles

[Based on 1203.3561, 1509.07637, 1712.07130, 1901.05370,....]

1. How near-extremal
are astrophysical
(Kerr) black holes?

AGNs are candidate High Spin Supermassive Black Holes

AGN	a	log M	$L_{\text{bol}}/L_{\text{Edd}}$	Host
MCG-6-30-15 ^a	$\geq +0.98$	$6.65^{+0.17}_{-0.17}$	$0.40^{+0.13}_{-0.13}$	E/S0
Fairall 9 ^b	$+0.52^{+0.19}_{-0.15}$	$8.41^{+0.11}_{-0.11}$	$0.05^{+0.01}_{-0.01}$	Sc
SWIFT J2127.4+5654 ^c	$+0.6^{+0.2}_{-0.2}$	$7.18^{+0.07}_{-0.07}$	$0.18^{+0.03}_{-0.03}$	—
1 H0707-495 ^d	$\geq +0.98$	$6.70^{+0.40}_{-0.40}$	$\sim 1.0_{-0.6}$	—
Mrk 79 ^e	$+0.7^{+0.1}_{-0.1}$	$7.72^{+0.14}_{-0.14}$	$0.05^{+0.01}_{-0.01}$	SBb
Mrk 335 ^f	$+0.70^{+0.12}_{-0.01}$	$7.15^{+0.13}_{-0.13}$	$0.25^{+0.07}_{-0.07}$	S0a
NGC 3783 ^g	$\geq +0.98$	$7.47^{+0.08}_{-0.08}$	$0.06^{+0.01}_{-0.01}$	SB(r)ab
Ark 120 ^h	$+0.94^{+0.1}_{-0.1}$	$8.18^{+0.05}_{-0.05}$	$0.04^{+0.01}_{-0.01}$	Sb/pec
3C 120 ⁱ	≥ 0.95	$7.74^{+0.20}_{-0.22}$	$0.31^{+0.20}_{-0.19}$	S0
1 H0419-577 ^j	$\geq +0.88$	$8.18^{+0.12}_{-0.12}$	$1.27^{+0.42}_{-0.42}$	—
Ark 564 ^j	$+0.96^{+0.01}_{-0.06}$	≤ 6.90	≥ 0.11	SB
Mrk 110 ^j	$\geq +0.99$	$7.40^{+0.09}_{-0.09}$	$0.16^{+0.04}_{-0.04}$	—
SWIFT J0501.9-3239 ^j	$\geq +0.96$	—	—	SB0/a(s) pec
Ton S180 ^j	$+0.91^{+0.02}_{-0.09}$	$7.30^{+0.60}_{-0.40}$	$2.15^{+3.21}_{-1.61}$	—
RBS 1124 ^j	$\geq +0.98$	8.26	0.15	—
Mrk 359 ^j	$+0.66^{+0.30}_{-0.54}$	6.04	0.25	pec
Mrk 841 ^j	$\geq +0.52$	7.90	0.44	E
IRAS 13224-3809 ^j	$\geq +0.995$	7.00	0.71	—
Mrk 1018 ^j	$+0.58^{+0.36}_{-0.74}$	8.15	0.01	S0
IRAS 00521-7054 ^l	$\geq +0.84$	—	—	—
NGC 4051 ^m	$\geq +0.99$	6.28	0.03	SAB(rs)bc
NGC 1365 ^k	$+0.97^{+0.01}_{-0.04}$	$6.60^{+1.40}_{-0.30}$	$0.06^{+0.06}_{-0.04}$	SB(s)b

7 out of 22
AGNs
observed in
X-rays
have

$$a > 0.98 M$$

[Brenneman, 2013]

(Controversy)

How High can the Spin be?

- Cosmic censorship conjecture: $a/M < 100\%$

- Thin disk accretion: $a/M < 99,8\%$

[Thorne, 1974]

- Accretion supported by magnetic fields: $< 100\%$

[Abramowicz, Lasota, 1980]



[0.9994 in Sadowski et al, 2011]

- Capture of compact objects: $< 100\%$

[Colleoni, Barack, Shah, van de Meent, 2015]

Population models and High Spin Supermassive black hole

For

$$M > 10^9 M_{\odot}$$

"Anisotropic accretion spins up the supermassive black hole to the Thorne bound"

[Berti, Volonteri, 2008]

→ Possibility for a High Spin Supermassive BH

2. Features at and close to extremality

2. Features at and close to extremality

Definition: at: $T_H = 0$

close to: $MT_H \ll 1$

Features of exactly extremal black holes

- $T_H = 0$
- Inner and outer horizons coincide.
NB: The inner horizon is unstable and singular.
[Marolf, "The dangers of extremes", 2010]
Breakdown of EFT: higher derivative and string corrections?
[Horowitz, Kolanowski, Remmen, Santos, 2023 and 2024]
- Most known are stationary, but non-stationary exist
[Murata, Reall, Tanahashi, 2013]
- No physical process is known that would make an extremal black hole from a non-extremal one. Third law of thermodynamics. [Mathematical fine-tuning is possible]
The reverse is possible.
- Stationarity implies axisymmetry assuming Einstein gravity + weak energy condition

Features of stationary extremal black holes

- Angular velocity from horizon generator: $\xi = \partial_t + \Omega_J \partial_\phi$
- Electrostatic potential: $\Phi_e = -\xi^\mu A_\mu |_{r=r_+}$
- If spin: ergoregion: ∂_t spacelike
- Superradiance: $0 < \omega < m\Omega_J$ (amplification due to lack of a global Killing vector). Negative greybody factor:
 $\sigma_{\text{abs}} = \frac{dE_{\text{abs}}/dt}{dE_{\text{in}}/dt} < 0$ in superradiant range.
Electromagnetic analogue in the range $0 < \omega < q_e \Phi_e$.
- No Hawking radiation but spontaneous emission of superradiant waves. Quantum decay.

$$\Gamma = \frac{1}{e^{\frac{\omega - m\Omega_J - q_e \Phi_e}{T_H}} - 1} \sigma_{\text{abs}}$$



$$\Gamma_{\text{ext}} = -\Theta(-\omega + m\Omega_J + q_e \Phi_e) \sigma_{\text{abs}}$$

Extremal Limits: the 4d Kerr example

"Several spacetimes can be obtained in a limit from a given spacetime, depending upon which coordinates are kept fixed during the limiting process"

[Geroch, Limits of spacetimes, 1970]

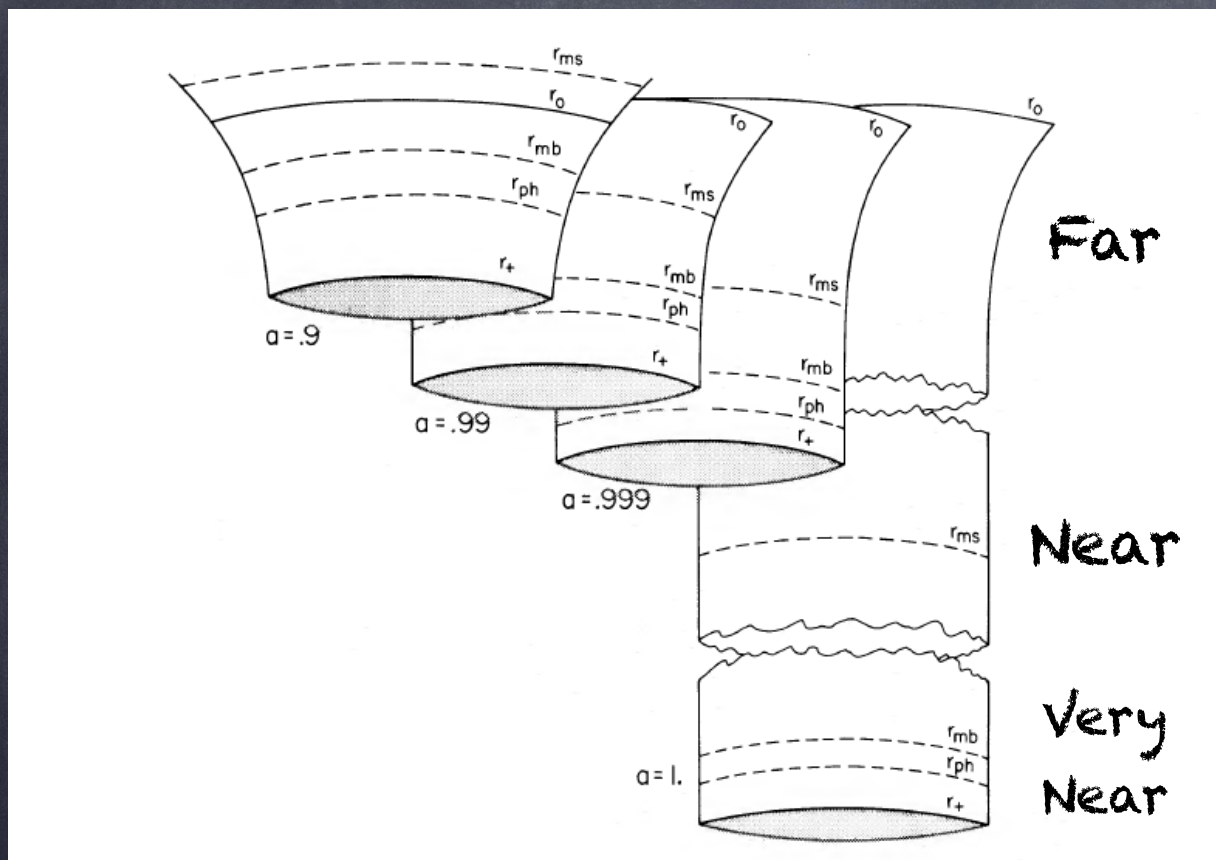
$$ds^2 = -\left(1 - \frac{2M\hat{r}}{\Sigma}\right)d\hat{t}^2 + \frac{\Sigma}{\Delta}d\hat{r}^2 + \Sigma d\theta^2 + \left(\hat{r}^2 + a^2 + \frac{2Ma^2\hat{r}\sin^2\theta}{\Sigma}\right)\sin^2\theta d\hat{\phi}^2 - \frac{4Ma\hat{r}\sin^2\theta}{\Sigma}d\hat{t}d\hat{\phi}$$

$$\Delta \equiv \hat{r}^2 - 2M\hat{r} + a^2, \quad \Sigma \equiv \hat{r}^2 + a^2 \cos^2\theta.$$

LIMIT 1) In Boyer-Lindquist coordinates, $\lambda \mapsto 0$ gives the Extremal Kerr metric.

Near-extremality

=> Opening up of "Near" and "Very Near" regions



- 1 Far region: extremal Kerr geometry
- 2 Near-horizon regions "Near" and "Very Near": NHEK geometry

[Bardeen, Press, Teukolsky, 1972]

[Bardeen, Horowitz, 1999]

The ISCO lies in the "Near" region

Feature: $\hat{r}_{ISCO} = M + 2^{1/3} \lambda^{2/3} M + O(\lambda)$

Change of coordinates to the "co-rotating near-horizon frame":

$$\begin{aligned} T &= \frac{\hat{t}}{2M} \lambda^{2/3}, \\ R &= \frac{\hat{r} - \hat{r}_+}{M} \lambda^{-2/3}, \\ \Phi &= \hat{\phi} - \Omega_{ext} \hat{t}, \quad \Omega_{ext} \equiv \frac{1}{2M}. \end{aligned}$$

LIMIT 2) Take $\lambda \mapsto 0$ in that frame: obtain the near-horizon extremal Kerr geometry (NHEK):

$$ds^2 = 2M^2 \Gamma(\theta) \left(-R^2 dT^2 + \frac{dR^2}{R^2} + d\theta^2 + \Lambda^2(\theta) (d\Phi + R dT)^2 \right)$$

$$\Gamma(\theta) = \frac{1 + \cos^2 \theta}{2}, \quad \Lambda(\theta) = \frac{2 \sin \theta}{1 + \cos^2 \theta}$$

NB: "ISCO is everywhere in NHEK" and "ISCO is at $R = 2^{1/3}$ "

Feature:

$$\hat{r}_{IBCO} = M + 2^{1/2}\lambda M + o(\lambda)$$

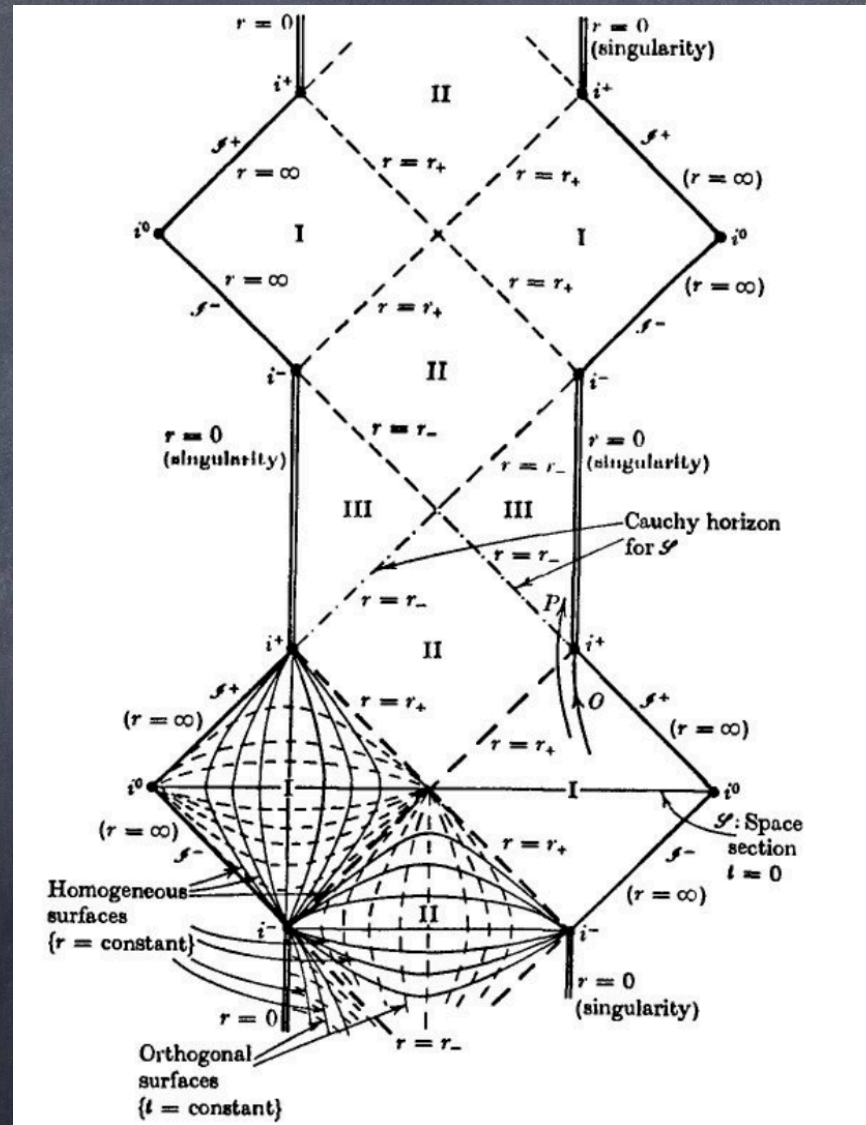
Change of coordinates to the "co-rotating very near-horizon frame":

$$\begin{aligned} t &= \frac{\hat{t}}{2M\kappa}\lambda, \\ r &= \kappa \frac{\hat{r} - \hat{r}_+}{M\lambda}, \\ \phi &= \hat{\phi} - \frac{\hat{t}}{2M}, \end{aligned}$$

LIMIT 3) Take $\lambda \mapsto 0$ in that frame: obtain the very near-horizon extremal Kerr geometry (near-NHEK):

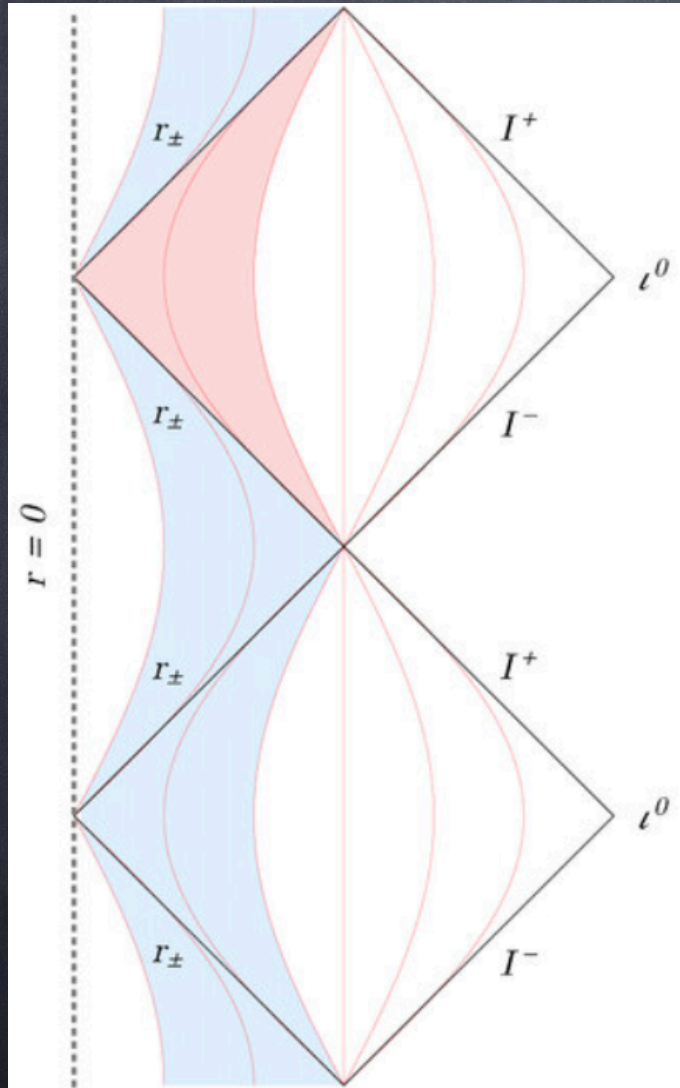
$$ds^2 = 2M^2\Gamma(\theta) \left(-r(r + 2\kappa)dt^2 + \frac{dr^2}{r(r + 2\kappa)} + d\theta^2 + \Lambda^2(\theta)(d\phi + (r + \kappa)dt)^2 \right)$$

Carter-Penrose diagram of non-extremal Kerr



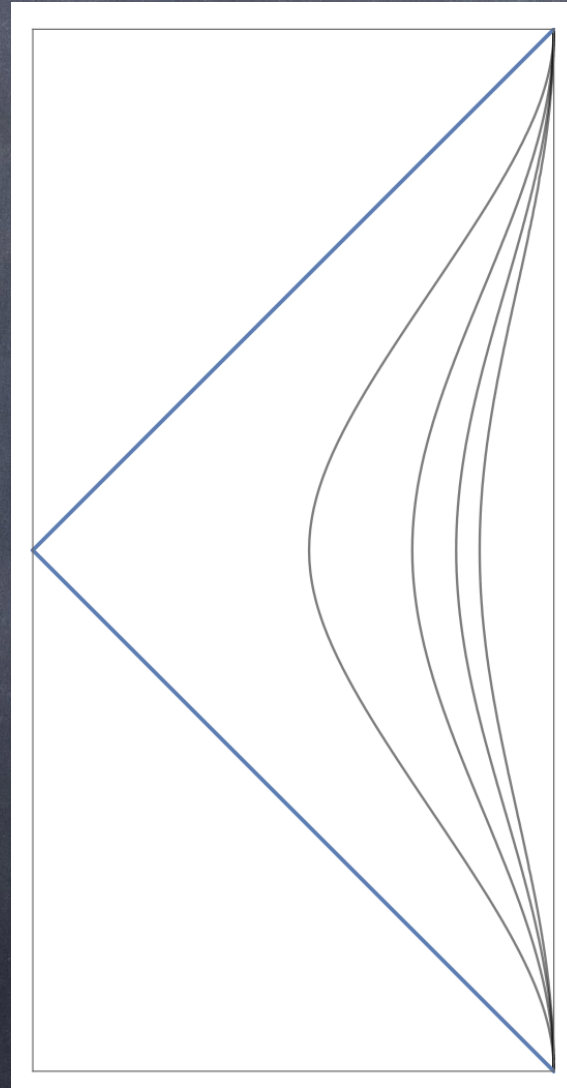
Penrose-Carter diagram of the 3 limiting spacetimes

Extremal Kerr



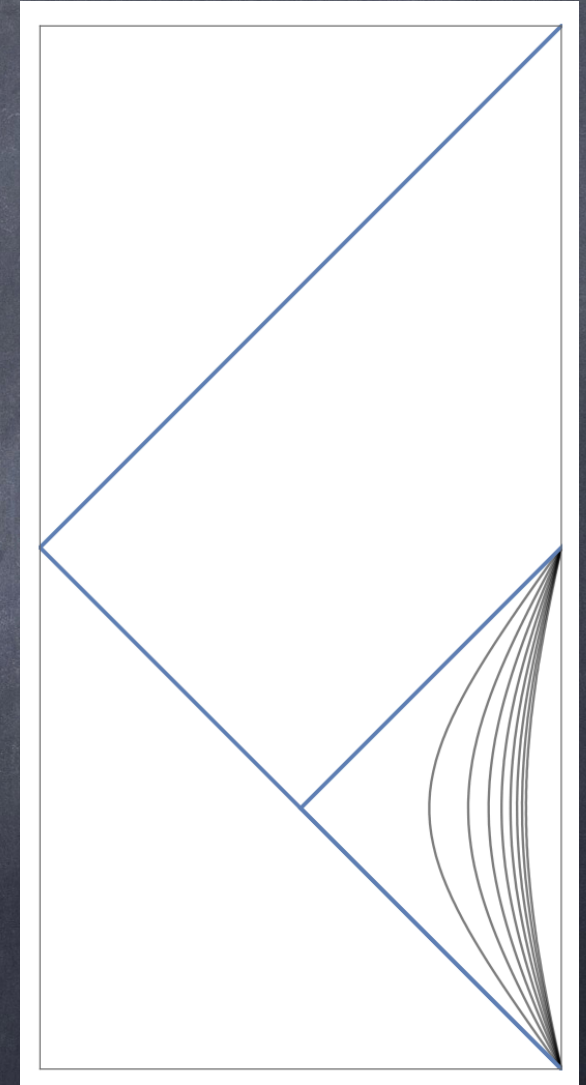
Exterior geodesics

NHEK



ISCO

near-NHEK



IBCO

Two finite diffeomorphisms

1. Finite diffeomorphism between NHEK and near-NHEK

$$\begin{aligned}R &= \frac{1}{\kappa} e^{\kappa t} \sqrt{r(r+2\kappa)}, \\T &= -e^{-\kappa t} \frac{r+\kappa}{\sqrt{r(r+2\kappa)}}, \\ \Phi &= \phi - \frac{1}{2} \log \frac{r}{r+2\kappa}.\end{aligned}$$

2. Finite diffeomorphism between NHEK and global NHEK coordinates

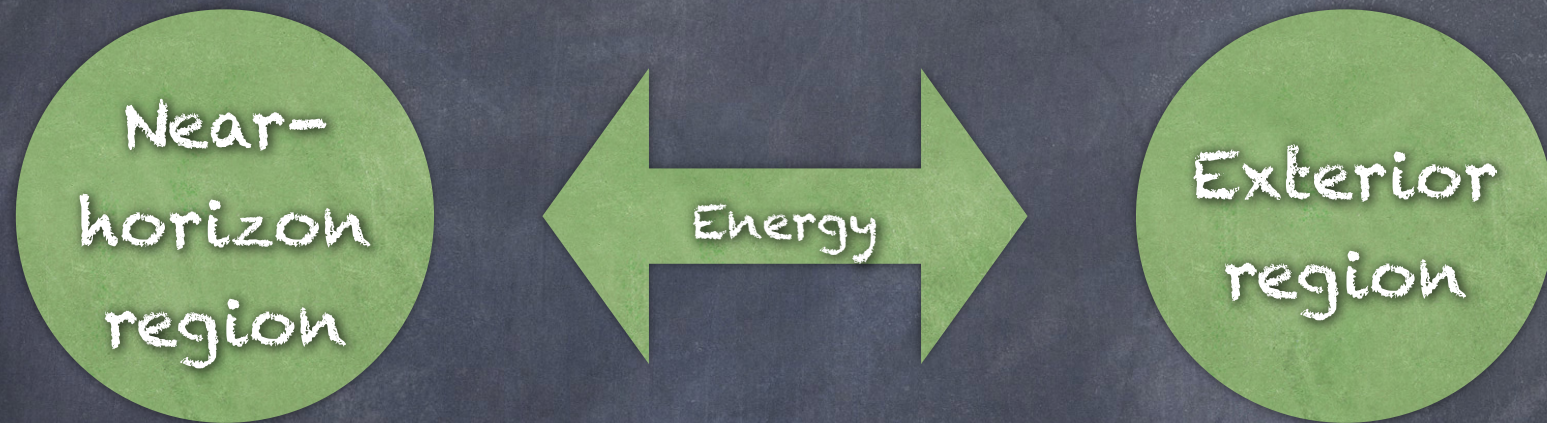
$$\begin{aligned}R &= \sqrt{1+y^2} \cos \tau + y, \\T &= \sqrt{1+y^2} \sin \tau \frac{1}{R}, \\ \Phi &= \varphi + \log \frac{\cos \tau + y \sin \tau}{1 + \sqrt{1+y^2} \sin \tau},\end{aligned}$$

$$ds^2 = 2M^2 \Gamma(\theta) \left(-(1+y^2) d\tau^2 + \frac{dy^2}{1+y^2} + d\theta^2 + \Lambda^2(\theta) (d\phi + y d\tau)^2 \right)$$

$$-\infty < \tau < \infty, \quad -\infty < y < \infty$$

Main feature of near-extremal black holes

Non-suppressed interactions between the near-horizon region and the environment



No Hamiltonian alone describes the evolution of the near-horizon region.

[Amsel, Horowitz, Marolf, Roberts, 2009]

[Dias, Reall, Santos, 2009]

Generic 4d near-horizon limits

Static Near-horizon Limit

$$t \rightarrow \frac{r_0 t}{\lambda}, \quad r \rightarrow r_+ + \lambda r_0 r,$$

+ Electric case: gauge transformation

Enhanced symmetry (by construction): $\zeta_0 = r\partial_r - t\partial_t$

Further enhancement to $SL(2, \mathbb{R})$ or $iso(1,1)$
[Kunduri, Lucietti, 2009, 2013]

Assuming strong energy condition, $SL(2, \mathbb{R})$!

Solution: $AdS_2 \times S^2$

$$ds^2 = v_1(-r^2 dt^2 + \frac{dr^2}{r^2}) + v_2(d\theta^2 + \sin^2 \theta d\phi^2),$$
$$\chi^A = \chi_*^A, \quad A^I = e_I r dt - \frac{p^I}{4\pi} \cos \theta d\phi,$$

Susy & non-susy: attractor mechanism: q^L, p^I rule it all.
May be walls of marginal stability in scalar moduli space.

Spinning Near-horizon Limit

$$t \rightarrow r_0 \frac{t}{\lambda},$$
$$r \rightarrow r_+ + \lambda r_0 r,$$

$$\phi \rightarrow \phi + \Omega_J^{\text{ext}} \frac{r_0 t}{\lambda},$$
$$A \rightarrow A + \frac{\Phi_e^{\text{ext}}}{\lambda} r_0 dt,$$

- + Spin case: corotate
- + Electric case: gauge transformation

Enhanced symmetry (by construction): $\zeta_0 = r\partial_r - t\partial_t$

Further enhancement to $SL(2, \mathbb{R})$ or $iso(1,1)$

[Kunduri, Lucietti, 2009, 2013]

Assuming strong energy condition, $SL(2, \mathbb{R})$!

Solution: warped $AdS_2 \times S^2$

$$ds^2 = \Gamma(\theta) \left[-r^2 dt^2 + \frac{dr^2}{r^2} + \alpha(\theta)^2 d\theta^2 + \gamma(\theta)^2 (d\phi + k r dt)^2 \right],$$

$$\chi^A = \chi^A(\theta), \quad A^I = f^I(\theta)(d\phi + k r dt) - \frac{e_I}{k} d\phi,$$

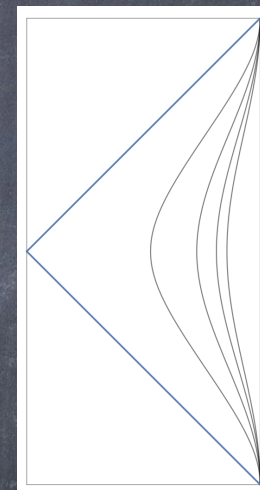
non-trivial gauge

Important feature: $SL(2, \mathbb{R}) \times U(1)$ symmetry

$$\begin{aligned} \zeta_{-1} &= \partial_t, & \zeta_0 &= t\partial_t - r\partial_r, \\ \zeta_1 &= \left(\frac{1}{2r^2} + \frac{t^2}{2} \right) \partial_t - t r \partial_r - \frac{k}{r} \partial_\phi, & L_0 &= \partial_\phi. \end{aligned}$$

In addition: discrete $(\mathbb{Z}_2)^3 = P \times r\phi \times t\phi$ symmetry

$$\begin{aligned} ds^2 &= \Gamma(\theta) \left[-r^2 dt^2 + \frac{dr^2}{r^2} + \alpha(\theta)^2 d\theta^2 + \gamma(\theta)^2 (d\phi + k r dt)^2 \right], \\ \chi^A &= \chi^A(\theta), & A^I &= f^I(\theta) (d\phi + k r dt) - \frac{e_I}{k} d\phi, \end{aligned}$$



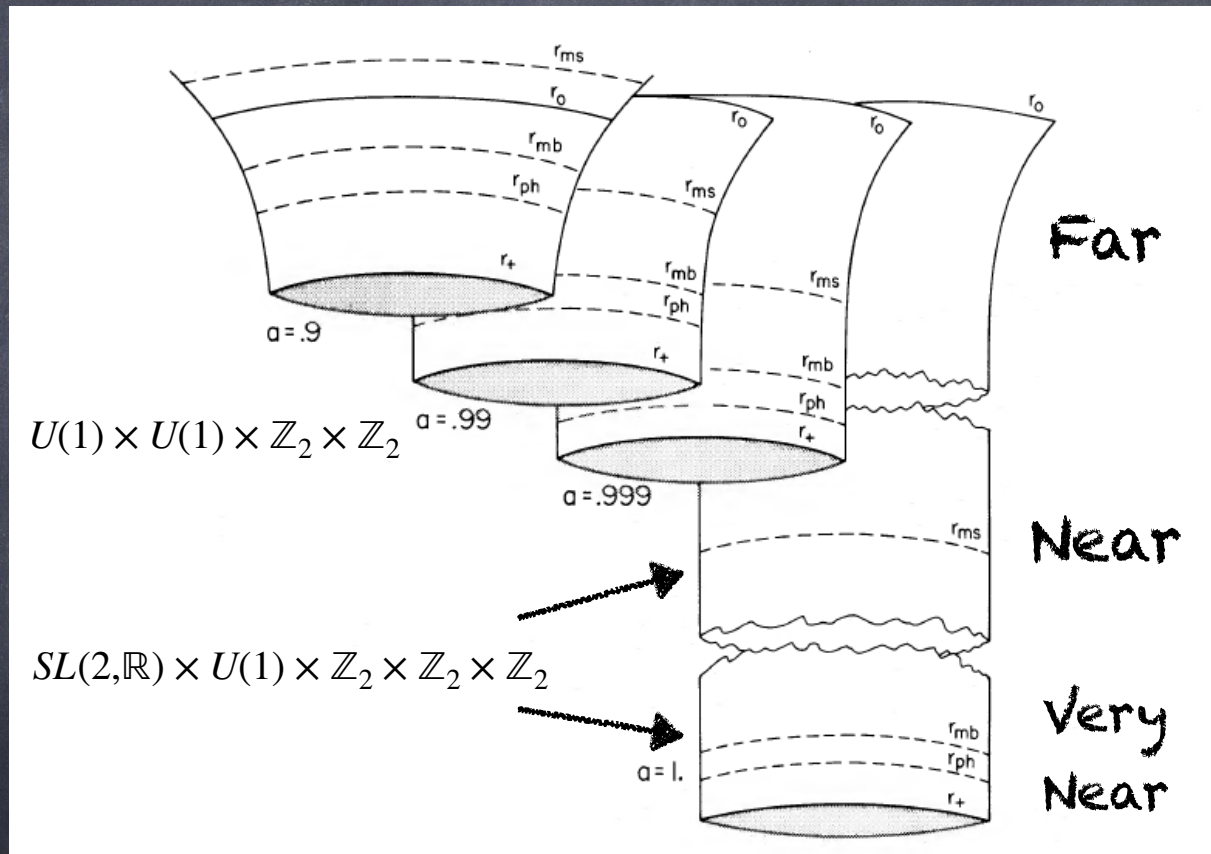
• Geodesic completeness expected (proven for Kerr)

• Global time function exists: no CTCs

$$g^{ab} \partial_a \tau \partial_b \tau = g^{\tau\tau} = -(1 + y^2)^{-1} \Gamma^{-1}(\theta) < 0$$

• No global Killing vector in general. No QFT vacuum [see Aggarwal's talk]

Extremality \Rightarrow Conformal symmetry



Other example: BTZ black hole

Extremal limit: $M\ell = \pm J$

The near-horizon limit gives

$$ds^2 = \frac{l^2}{4} \left(-r^2 dt^2 + \frac{dr^2}{r^2} + 2|\mathcal{J}| \left(d\phi + \frac{r}{\sqrt{2|\mathcal{J}|}} dt \right)^2 \right)$$

This is the self-dual AdS_3 orbifold

[Coussaert, Henneaux, 1994]

There also exist singular near-horizon geometries

- Obtained in the limit $T_H \mapsto 0$ and $A_{BH} \mapsto 0$ keeping A_{BH}/T_H fixed.
- Contain an AdS_3 factor: either a null self-dual orbifold or a pinching orbifold

[Bardeen, Horowitz, 1999][Balasubramanian, de Boer, Jejjala, Simon, 2008][de Boer, Sheikh-Jabbari, Simon, 2010]

Thermodynamics at extremality

Stationary black hole entropy formula [Iyer-Wald, 1994]:

$$S = \frac{1}{4G_N \hbar} \int_{\Sigma} \text{vol}(\Sigma),$$

$$S = -\frac{2\pi}{\hbar} \int_{\Sigma} \frac{\delta^{\text{cov}} L}{\delta R_{abcd}} \epsilon_{ab} \epsilon_{cd} \text{vol}(\Sigma)$$

Attractor mechanism: the entropy is the extremum of

$$\mathcal{E}(\Gamma(\theta), \alpha(\theta), \gamma(\theta), f^I(\theta), \chi^A(\theta), k, e_I) = 2\pi(k\mathcal{J} + e_I Q^I - \int_{\Sigma} d\theta d\phi \sqrt{-g} \mathcal{L}),$$

$$\frac{\delta \mathcal{E}}{\delta \Gamma(\theta)} = \frac{\delta \mathcal{E}}{\delta \alpha(\theta)} = \frac{\delta \mathcal{E}}{\delta \gamma(\theta)} = \frac{\delta \mathcal{E}}{\delta f^I(\theta)} = \frac{\delta \mathcal{E}}{\delta \chi^A(\theta)} = \frac{\delta \mathcal{E}}{\delta k} = \frac{\delta \mathcal{E}}{\delta e_I} = 0$$

Entropy is a function of the charges (only discontinuous dependency on scalar moduli):

$$S = S_{\text{ext}}(\mathcal{J}, Q_e^I, Q_m^I)$$

[Sen, 2005]

Logarithmic corrections can be computed (one method: the quantum entropy action formalism) [Sen, 2011]

Such quantum corrections might lift the vacuum degeneracy at extremality in the absence of protective symmetries [Page, 2000]
[See talk of Swapnamay Mondal]

Some diffeomorphisms were identified in the near-horizon limit become zero modes that contribute to the gravitational path integral [Ghosh, Maxfield, Turiaci, 2019]

Such modes are computed using an IR regulator T_q .

For Kerr this gives [Rakic, Rangamani, Turiaci, 2024] [Kapec, Sheta, Strominger, Toldo, 2023]

$$S = S_0 + \frac{154}{180} \log S_0 + 4\pi^2 \frac{T}{T_q} + \frac{3}{2} \log \frac{T}{T_q} + \mathcal{O}(T^2).$$

$$e^{-S_0 T_q} \lll T \lll T_q$$

The zero modes lower the entropy, which might be consistent with a zero entropy in the extremal limit.

Extremal first law of thermodynamics

Given the entropy function $S = S_{\text{ext}}(\mathcal{J}, Q_e^I, Q_m^I)$ we define the chemical potentials:

$$\frac{1}{T_\phi} = \left(\frac{\partial S_{\text{ext}}}{\partial \mathcal{J}} \right)_{Q_e, m}, \quad \frac{1}{T_e} = \left(\frac{\partial S_{\text{ext}}}{\partial Q_e} \right)_{\mathcal{J}, Q_m}, \quad \frac{1}{T_m} = \left(\frac{\partial S_{\text{ext}}}{\partial Q_m} \right)_{\mathcal{J}, Q_e}$$

They obey

$$\delta S_{\text{ext}} = \frac{1}{T_\phi} \delta \mathcal{J} + \frac{1}{T_e} \delta Q_e + \frac{1}{T_m} \delta Q_m$$

This is the extremal limit of the first law :

$$\delta S = \frac{1}{T_H} (\delta M - (\Omega_J \delta \mathcal{J} + \Phi_e \delta Q_e + \Phi_m \delta Q_m))$$

$$\delta M = \delta M_{\text{ext}}(\mathcal{J}, Q_e, Q_m)$$

The chemical potentials are now obtained from a limit:

$$T_\phi = \lim_{T_H \rightarrow 0} \frac{T_H}{\Omega_J^{\text{ext}} - \Omega_J} = - \left. \frac{\partial T_H / \partial r_+}{\partial \Omega_J / \partial r_+} \right|_{r_+ = r_{\text{ext}}},$$
$$T_{e,m} = \lim_{T_H \rightarrow 0} \frac{T_H}{\Phi_{e,m}^{\text{ext}} - \Phi_{e,m}} = - \left. \frac{\partial T_H / \partial r_+}{\partial \Phi_{e,m} / \partial r_+} \right|_{r_+ = r_{\text{ext}}},$$

Laws of thermodynamics of extremal black holes

- The extremal limit of the first law

$$\delta\mathcal{S}_{\text{ext}} = \frac{1}{T_\phi}\delta\mathcal{J} + \frac{1}{T_e}\delta Q_e + \frac{1}{T_m}\delta Q_m.$$

- The zero law (with $SL(2, \mathbb{R})$ symmetry)

$$T_\phi = \frac{1}{2\pi k}, \quad T_e = \frac{1}{2\pi e}$$

- "Classical" extremal entropy = extremum of the entropy function

$$\mathcal{E} \equiv \frac{\mathcal{J}}{T_\phi} + \frac{Q_e}{T_e} + \frac{Q_m}{T_m} - 2\pi \int_\Sigma d\theta d\phi \sqrt{-g} \mathcal{L},$$

[Astefanesei, Goldstein, Jena, Sen, Trivedi, 2006]

[Hajian, Seraj, Sheikh-Jabbari, 2013]

Kerr/CFT entropy match

1) Ansatz: asymptotic symmetry generator

$$\zeta_\epsilon = \epsilon(\varphi)\partial_\varphi - r\epsilon'(\varphi)\partial_r .$$

$$\epsilon_n(\varphi) = -e^{-in\varphi}$$

$$\zeta_n = \zeta(\epsilon_n)$$

$$i[\zeta_m, \zeta_n]_{L.B.} = (m - n)\zeta_{m+n}$$

2) Phase space: empty, except finite diffeomorphisms !

3) Associated asymptotic symmetry algebra

$$[L_m, L_n] = (m - n)L_{m+n} + \frac{J}{\hbar}m(m^2 - 1)\delta_{m+n,0}.$$

$$c_L = \frac{12J}{\hbar}$$

4) "Thermal" Cardy formula

$$S = \frac{\pi^2}{3}c_L T_L$$

5) Entropy matching

$$S_{micro} = \frac{2\pi J}{\hbar} = S_{BH}$$

Extremal entropy matching

$$\frac{\pi^2}{3} c_L T_L = S_{BH}$$

Matching is (surprisingly!) very general:

- Gauge fields, scalar fields
- Higher dimensions
- Supergravities
- Higher derivative corrections

Higher derivative corrections to black hole entropy

A diffeomorphic covariant Lagrangian for the metric can be written as

$$L = \star f(g_{ab}, R_{abcd}, \nabla_{e_1} R_{abcd}, \nabla_{(e_1} \nabla_{e_2)} R_{abcd}, \dots, \nabla_{(e_1} \dots \nabla_{e_k)} R_{abcd}),$$

$$\begin{aligned} L = \star & [f(g_{ab}, \mathbb{R}_{abcd}, \mathbb{R}_{abcd|e_1}, \dots, \mathbb{R}_{abcd|e_1 \dots e_k}) + Z^{abcd}(R_{abcd} - \mathbb{R}_{abcd}) \\ & + Z^{abcd|e_1}(\nabla_{e_1} \mathbb{R}_{abcd} - \mathbb{R}_{abcd|e_1}) + Z^{abcd|e_1 e_2}(\nabla_{(e_2} \mathbb{R}_{abcd|e_1)} - \mathbb{R}_{abcd|e_1 e_2}) \\ & + \dots + Z^{abcd|e_1 \dots e_k}(\nabla_{(e_k} \mathbb{R}_{abcd|e_1 \dots e_{k-1}}) - \mathbb{R}_{abcd|e_1 \dots e_k})]. \end{aligned}$$

[Lee, Iyer, Wald, 1990]

The stationary black hole entropy is

$$S = -\frac{2\pi}{\hbar} \int_{\Sigma} \frac{\delta^{\text{cov}} L}{\delta R_{abcd}} \epsilon_{ab} \epsilon_{cd} \text{vol}(\Sigma).$$

$$\frac{\delta^{\text{cov}}}{\delta R_{abcd}} = \sum_{i=0} (-1)^i \nabla_{(e_1} \dots \nabla_{e_i)} \frac{\partial}{\partial \nabla_{(e_1} \dots \nabla_{e_i)} R_{abcd}}.$$

[Iyer-Wald, 1993]

Higher derivative corrections to black hole entropy

Metric with $SL(2, \mathbb{R}) \times U(1) \times t - \phi$ symmetry

$$ds^2 = A(\theta)^2 \left(-r^2 dt^2 + \frac{dr^2}{r^2} \right) + d\theta^2 + B(\theta)^2 (d\varphi + kr dt)^2.$$

Ansatz for asymptotic symmetry:

$$\xi_n = -e^{-in\varphi} (\partial_\varphi + inr \partial_r),$$

$$i[\xi_m, \xi_n] = (m - n)\xi_{m+n}.$$

Representation by charges:

$$i\{H_m, H_n\} = (m - n)H_{m+n} + \frac{c}{12} m(m^2 + a)\delta_{m,-n},$$

$$\frac{c}{12} m(m^2 + a)\delta_{m,-n} = i \int_{\Sigma} \mathbf{k}_{\xi_m} [\delta_{\xi_n} g; g],$$

The Barnich-Brandt definition for \mathbf{k}_{ξ_m} reproduces the formula

$$\frac{\pi^2}{3} cT = S,$$

[Azeyanagi, Compère, Ozawa, Tachikawa, Terashima, 2009]

Puzzle: non-invariance under field redefinition. Boundary terms?

[Krishnan, Kuperstein, 2009] [H-S. Liu, H. Lü, 2021]

Puzzle: non-uniqueness of Virasoro central charge

Ansatz for asymptotic symmetries:

$$\bar{\chi}[\epsilon(\vec{\varphi})] = \epsilon \vec{k} \cdot \vec{\partial}_\varphi - \vec{k} \cdot \vec{\partial}_\varphi \epsilon \left(\frac{b}{r} \partial_t + r \partial_r \right)$$

Regularity of the constant t, r surfaces fixes $b = \pm 1$ instead of $b = 0$. This leads to a smooth phase space of geometries.

The asymptotic symmetry algebra is

$$\{H_{\vec{m}}, H_{\vec{n}}\} = -i \vec{k} \cdot (\vec{m} - \vec{n}) H_{\vec{m}+\vec{n}} + C_{\vec{m},\vec{n}}$$

$$iC_{\vec{m},\vec{n}} = (\vec{k} \cdot \vec{m})^3 \left((1 - b(b + \Delta)) \frac{A_{\mathcal{H}}}{8\pi G} + 2b(b + \Delta) \vec{k} \cdot \vec{J} \right) \delta_{\vec{m}+\vec{n},0} \\ + (\vec{k} \cdot \vec{m}) (2\vec{k} \cdot \vec{J}) \delta_{\vec{m}+\vec{n},0}$$

Observational features of High Spin

Caveat: Extremely high spin

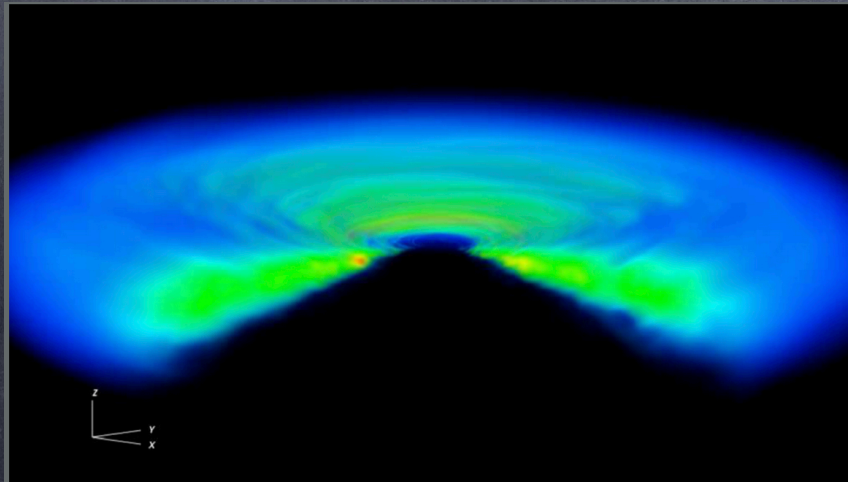
$$a > 0.9999 M$$

is generally required in order that
the NHEK features dominate
at least part of the signal

1) Cold accretion disk

The standard Novikov-Thorne model assumes :

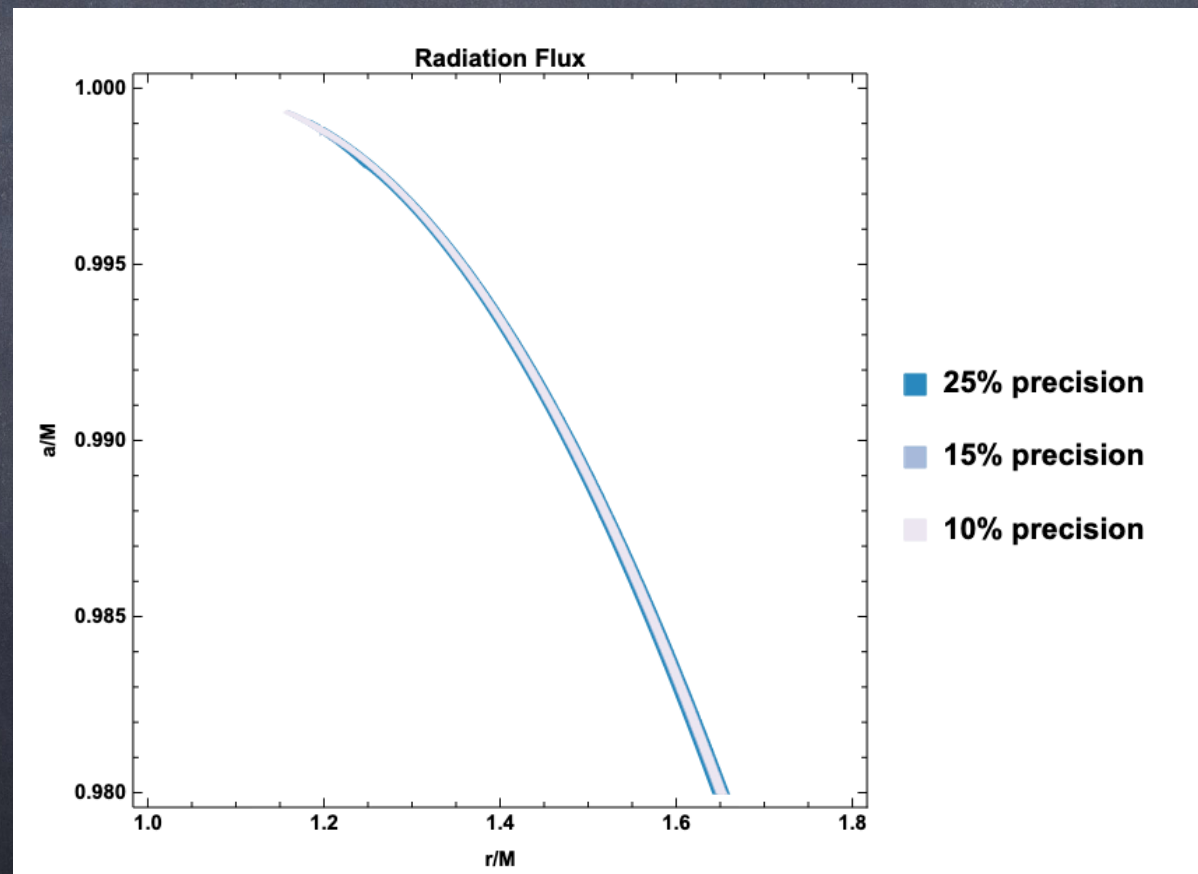
- Relativistic viscous fluid flow (relativistic Navier-Stokes)
- Thermal equilibrium ($T \sim 10^4 - 10^7 K$ lower than virial T)
- Geometrically thin disk
- Optically thick disk (free-free electrons absorption and electron scattering) with radiating EM flux
- Radiation pressure and gas pressure



Volume visualization of the logarithmic density in the accretion disk
(Teixeira et al. 2013)

The extremal limit of the Novikov-Thorne model is a self-similar solution.

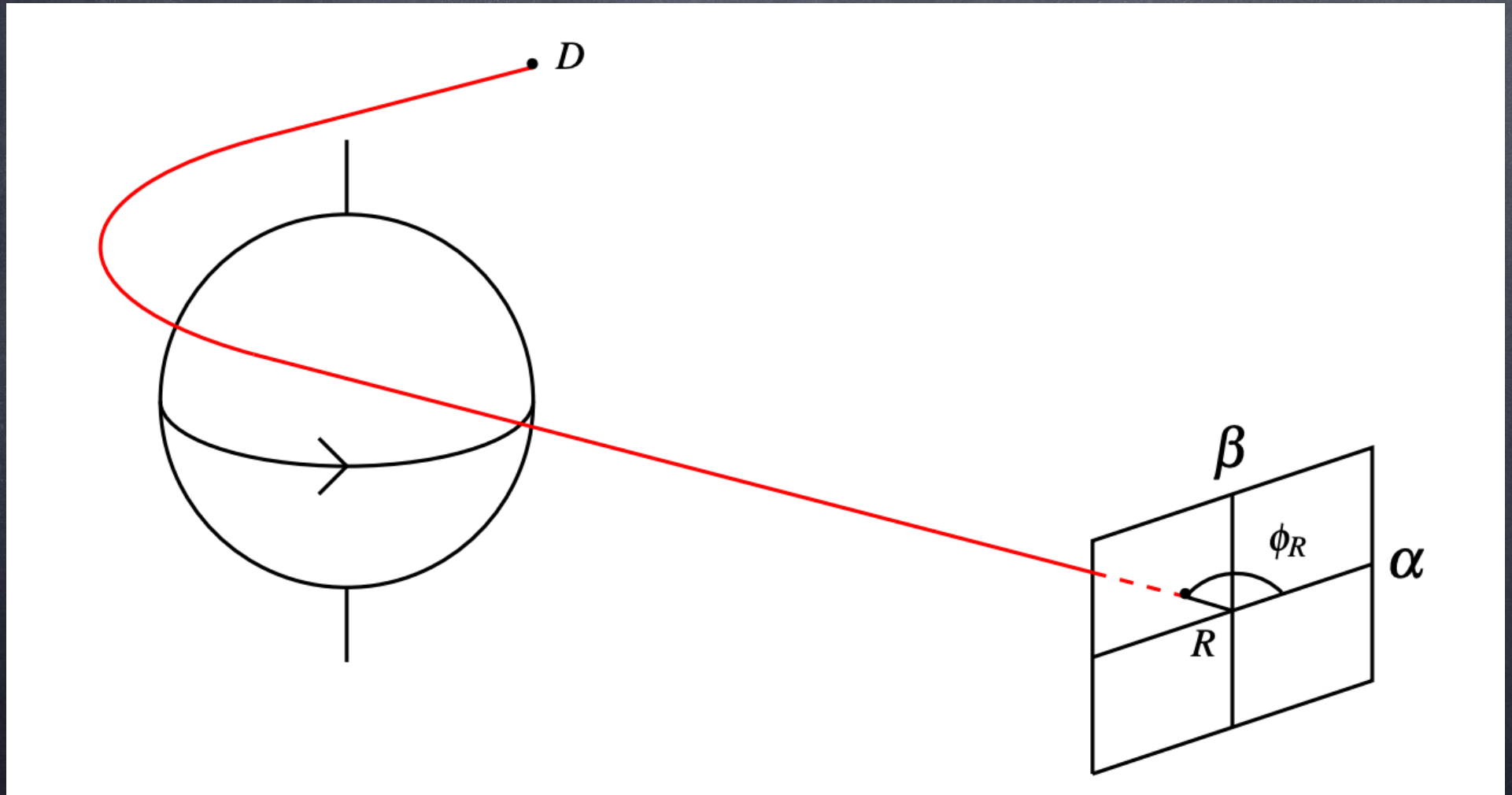
However, the NHEK features are barely visible



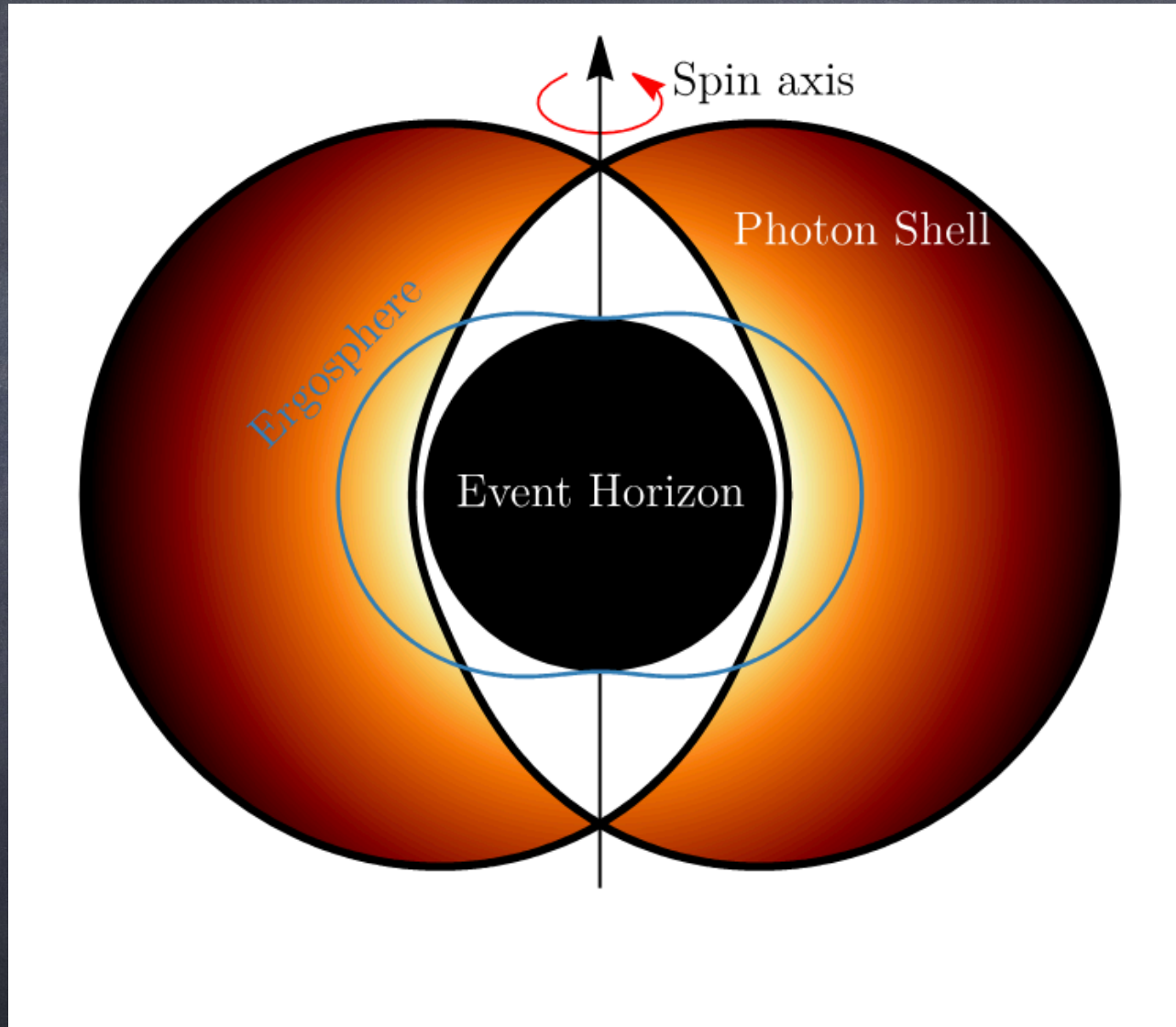
[Compère, Oliveri, 2017]

2) Black hole imaging

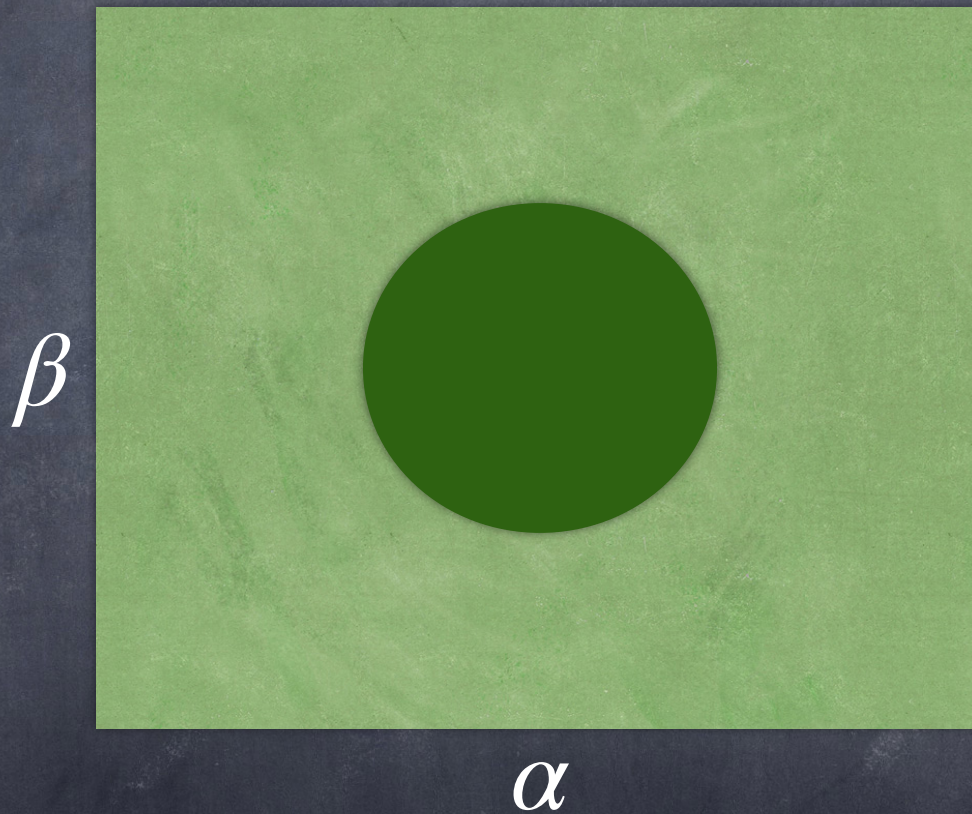
Bardeen screen



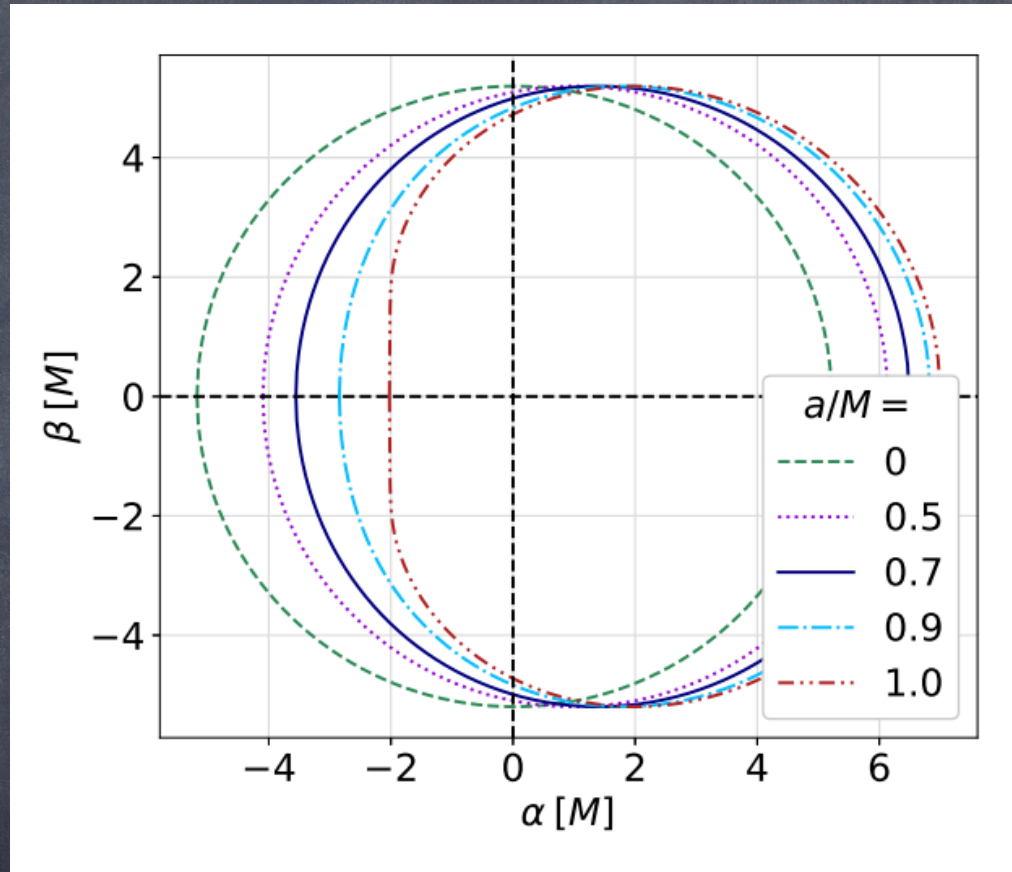
Photon shell



Critical curve

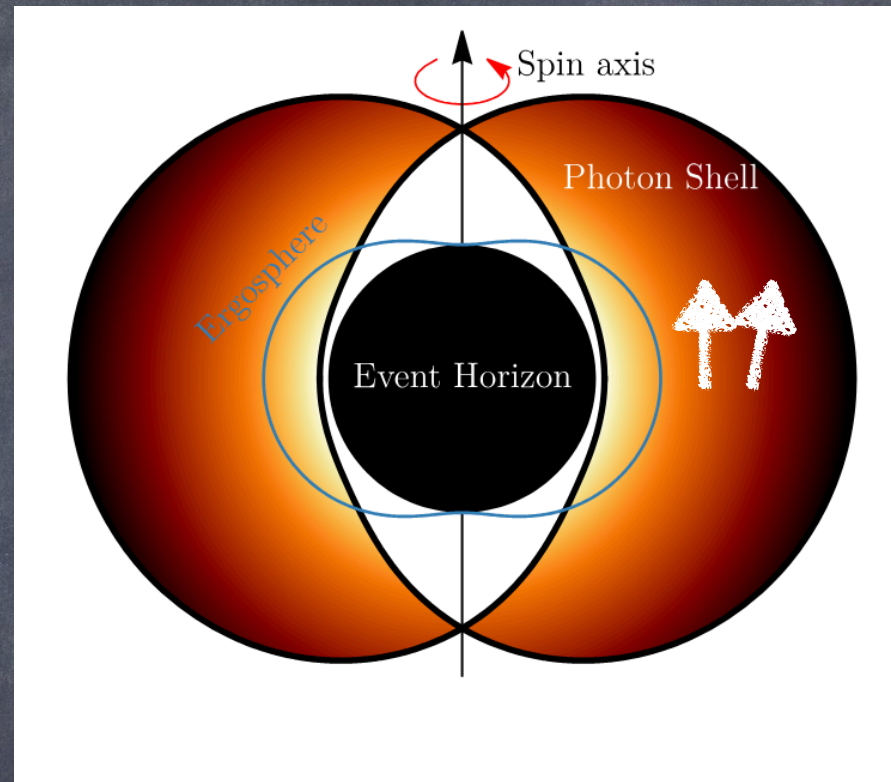


At extremality, the critical curve contains the NHEK line



[Bardeen, 1973] [Gralla, Lupsasca, Strominger, 2017] [Lupsasca, Porfyriadis, Shi, 2017] [Lupsasca, Mayerson, Ripperda, Staelens, 2024]

Lyapunov exponents of the critical curve

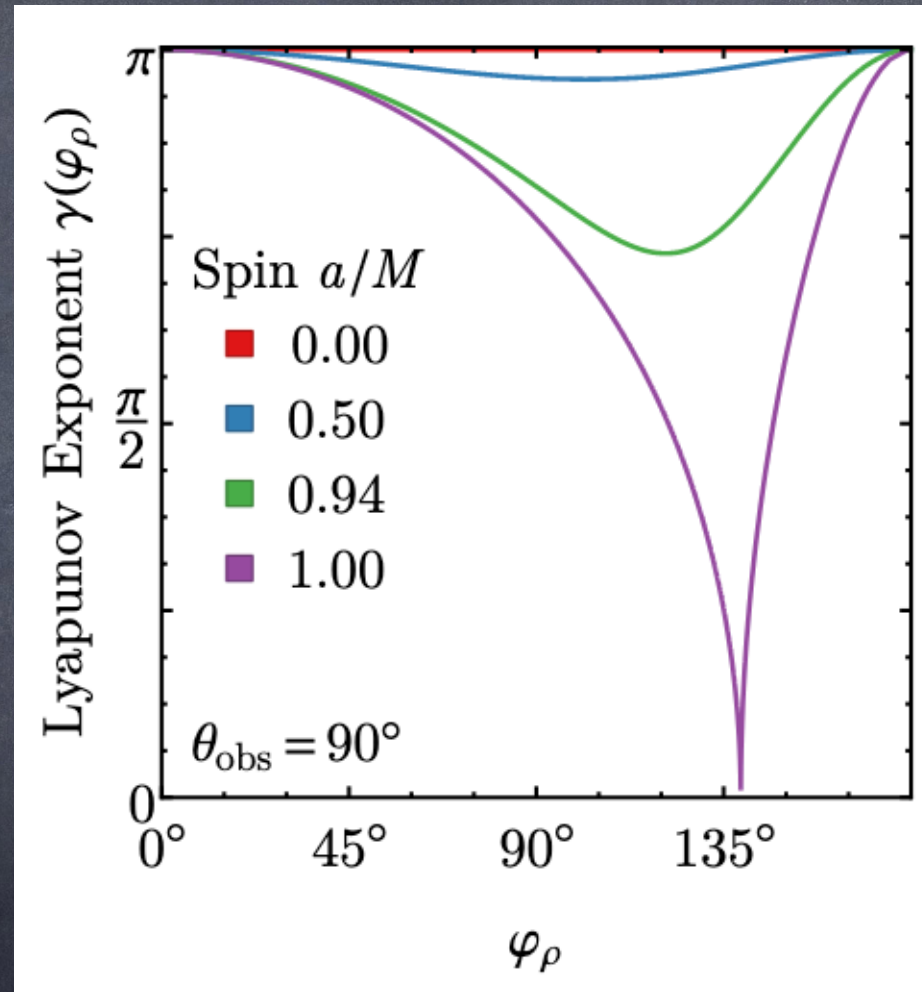


Nearly critical null geodesics have exponential deviation in their radius:

$$\delta r_n = \delta r e^{\gamma n}$$

where n is the number of half-orbits and $\gamma(a, r)$ is a critical exponent.

Lyapunov exponents of the critical curve



There are 3 other characteristic Lyapunov exponents

[Lupsasca, Porfyriadis, Shi, 2017] [Johnson et al. 2019]

Observability

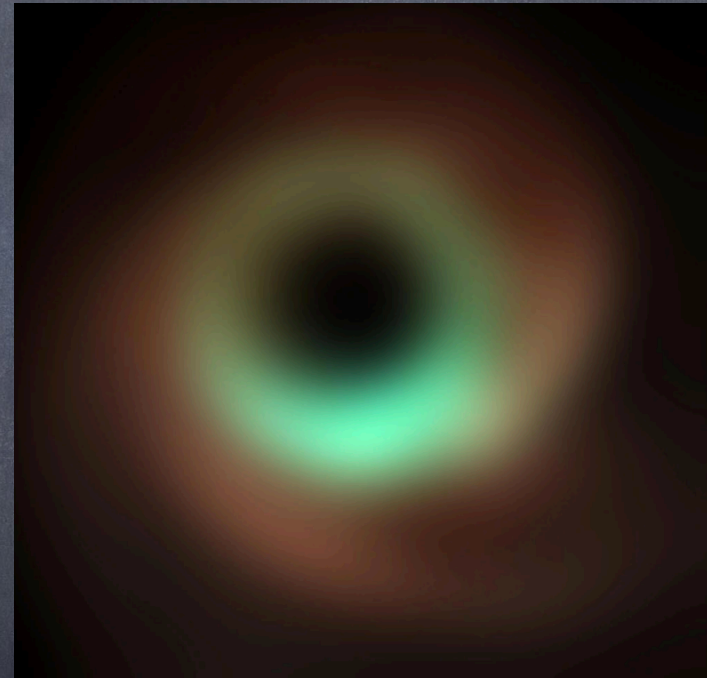
Event Horizon Telescope



Observability

Only a handful of sources :

- Sgr A*
- M87*
- ...



345 GHz

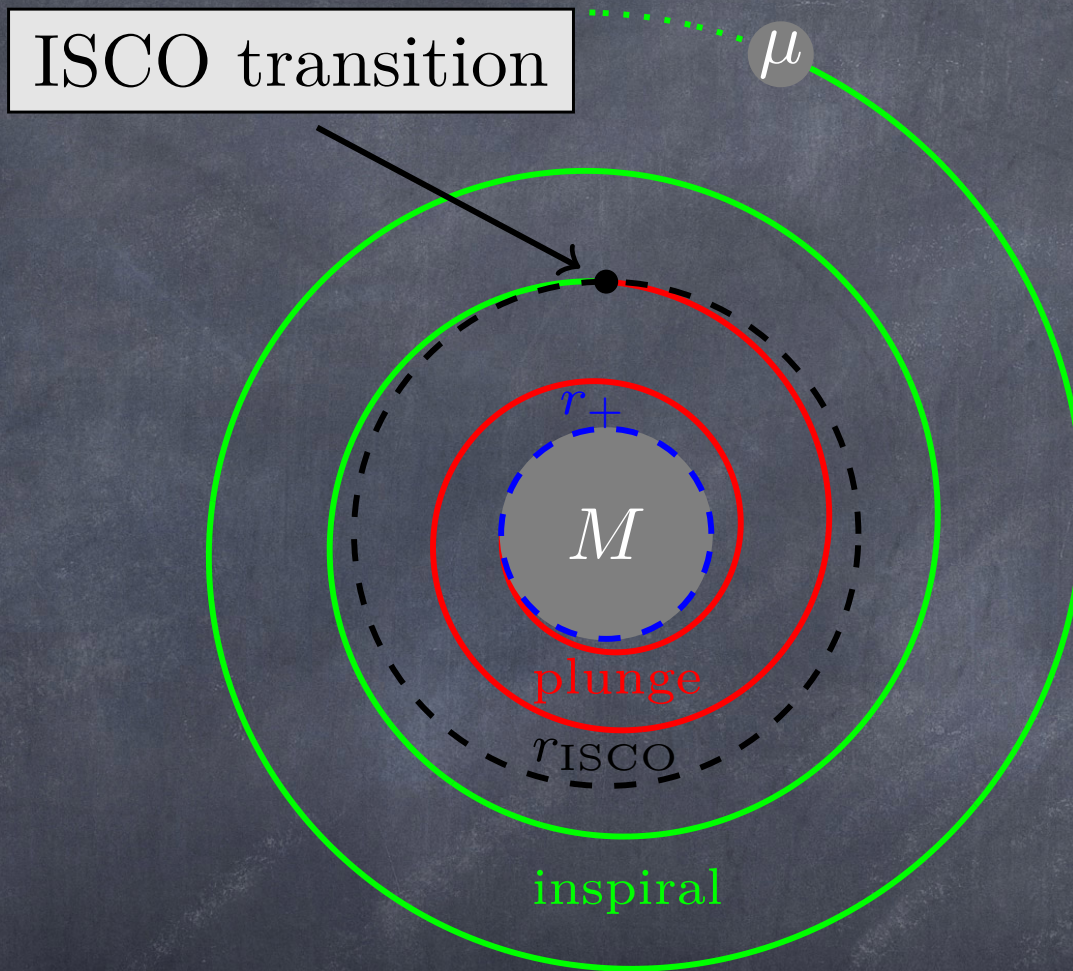
Low probability of high spin $a > 0.999$

3) Gravitational waves

Binary coalescences:

- 2G - LVK : LIGO-Virgo-Kagra
- 3G - Einstein Telescope
- 3G - Cosmic Explorer
- 3G - LISA

Stages of a coalescence around a High Spin black hole



Smoking Gun #1

Locked oscillation timescale

- The ISCO is in the Near Horizon region. The adiabatically evolved inspiral/merger as well.
- The Near Horizon region is exactly co-rotating with the Black hole
- Hence, the GW oscillation timescale of inspirals/plunges in NHEK is fixed to the inverse extremal Kerr angular velocity:

$$\hat{t}_{oscillation} = \Omega_{Ext}^{-1} = 2GM$$

Smoking Gun #2

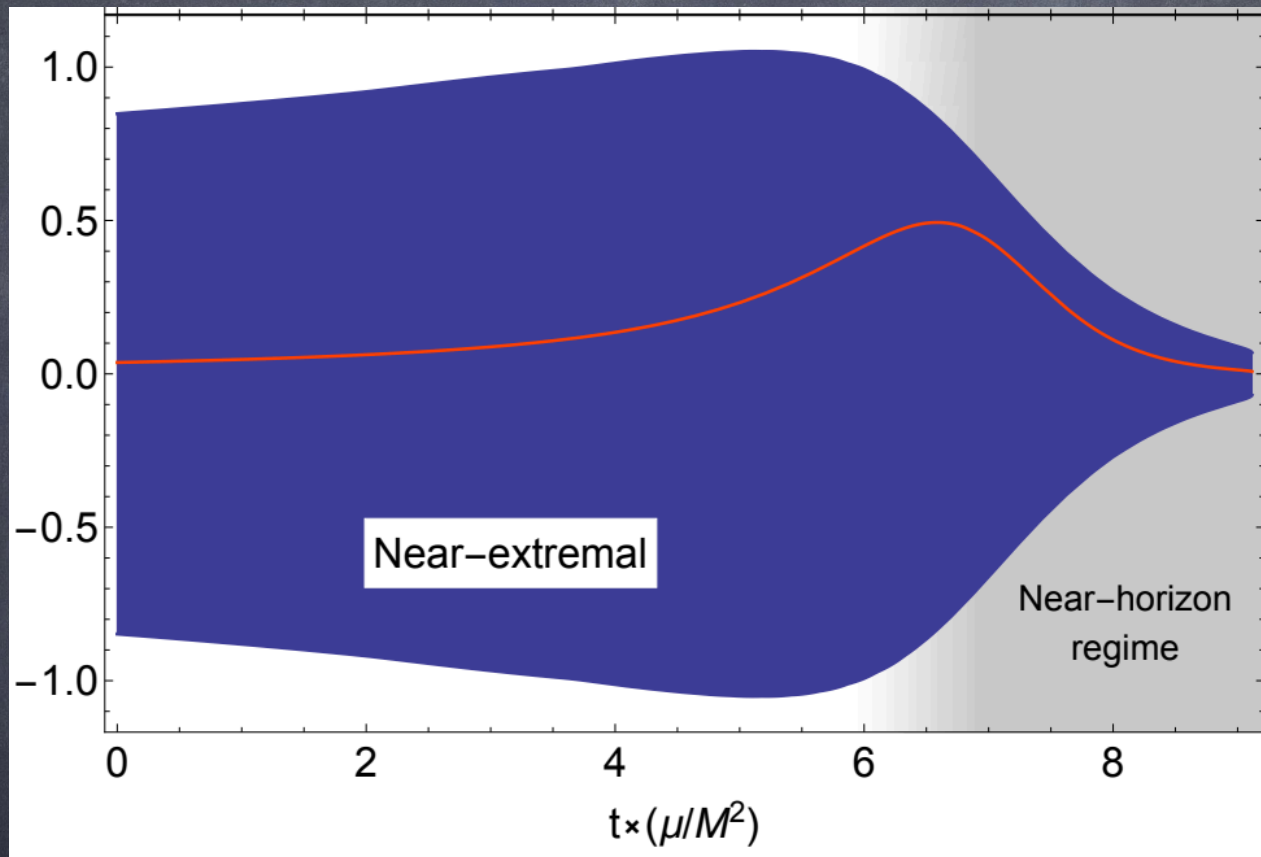
Redshift suppression

- The ISCO is in the Near Horizon Region which is redshifted.
- The GW amplitude is therefore suppressed.
The scaling is universally

$$|h_+ + ih_\times| \sim \lambda^{1/3} e^{-t/\tau}$$
$$\tau = 0.451\mu \left(\frac{M}{\mu}\right)^2 \quad \lambda = \sqrt{1 - \frac{a^2}{m^2}}$$

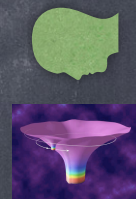
Resulting inspiral waveform

h_+



$$a/M = 1 - 10^{-9}$$

Face-on



[Gralla, Hughes, Warburton, 2016]

GW fluxes for a NHEK circular orbit: spin and finite size corrections

$$\left(\frac{dE}{d\hat{t}}\right)^\infty = q^2 \hat{x}_0 (a_{(0)}^\infty + a_{(1)}^\infty \chi q + (a_{(2)}^\infty + \tilde{a}_{(2)}^\infty \kappa_S^2)(\chi q)^2 + O(q^3));$$

$$\left(\frac{dE}{d\hat{t}}\right)^H = q^2 \hat{x}_0 (a_{(0)}^H + a_{(1)}^H \chi q + (a_{(2)}^H + \tilde{a}_{(2)}^H \kappa_S^2)(\chi q)^2 + O(q^3))$$

where $\hat{x}_0 = (2\lambda^2)^{1/3}$ and

$$q \equiv \frac{\mu}{M} \ll 1.$$

$$\chi \equiv \frac{S}{\mu^2}$$

$$\begin{aligned} a_{(0)}^\infty &= 0.987; & a_{(0)}^H &= -0.13285; \\ a_{(1)}^\infty &= -0.409; & a_{(1)}^H &= 0.28780; \\ a_{(2)}^\infty &= 0.784; & a_{(2)}^H &= -0.03169; \\ \tilde{a}_{(2)}^\infty &= 2.889; & \tilde{a}_{(2)}^H &= -0.70616. \end{aligned}$$

Point Particle: [Gralla, Hughes, Warburton, 2016]

Spin-spin couplings and spin-induced quadrupole coupling: [Chen, Compère, Liu, Long, Zhang, 2019]

Observability by LISA

We need an intermediate mass black hole coalescing into a high spin supermassive BH within $(1 \text{ Gpc})^3$

$$D^{max} \approx 1 \text{ Gpc} \left(\frac{M}{10^7 M_{\odot}} \right)^{1/2} \left(\frac{\mu}{100 M_{\odot}} \right) \left(\frac{15}{SNR} \right)$$

[Gralla, Hughes, Warburton, 2016]

[Compère, Fransen, Hertog, Long, 2018]

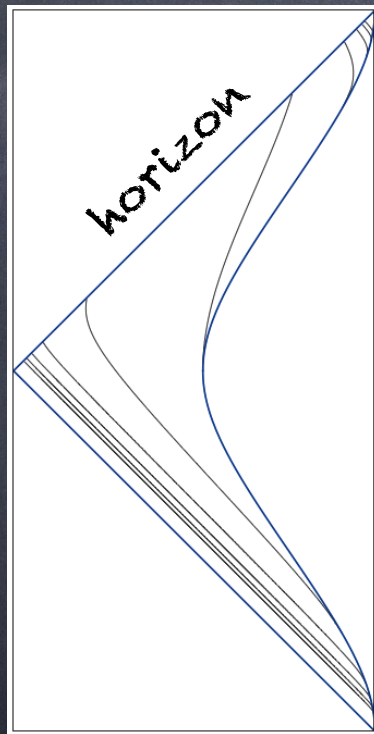
[Burke, Gair, Simon, Edwards, 2020]

Motivation: A small black hole orbiting a supermassive black hole follows a sequence of geodesics.

Near-horizon Kerr Geodesics

Feature: Critical proper angular momentum

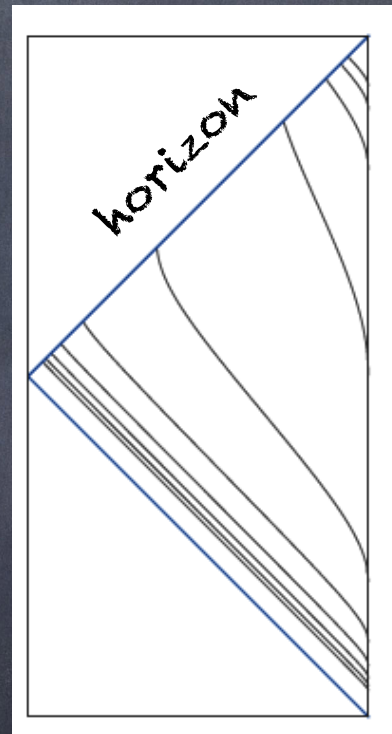
$$l_* = \frac{\hat{E}_{ISCO}}{\Omega_{ext}} = \frac{2}{\sqrt{3}} M$$



Matching region

Subcritical orbits

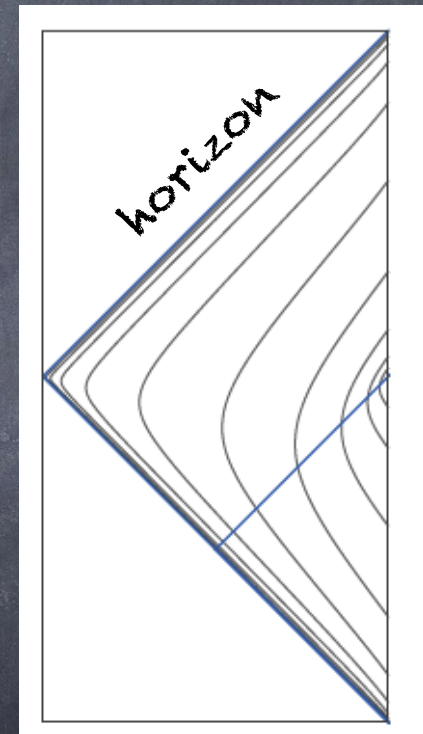
$$l < l_*$$



Matching region

Critical orbits

$$l = l_*$$

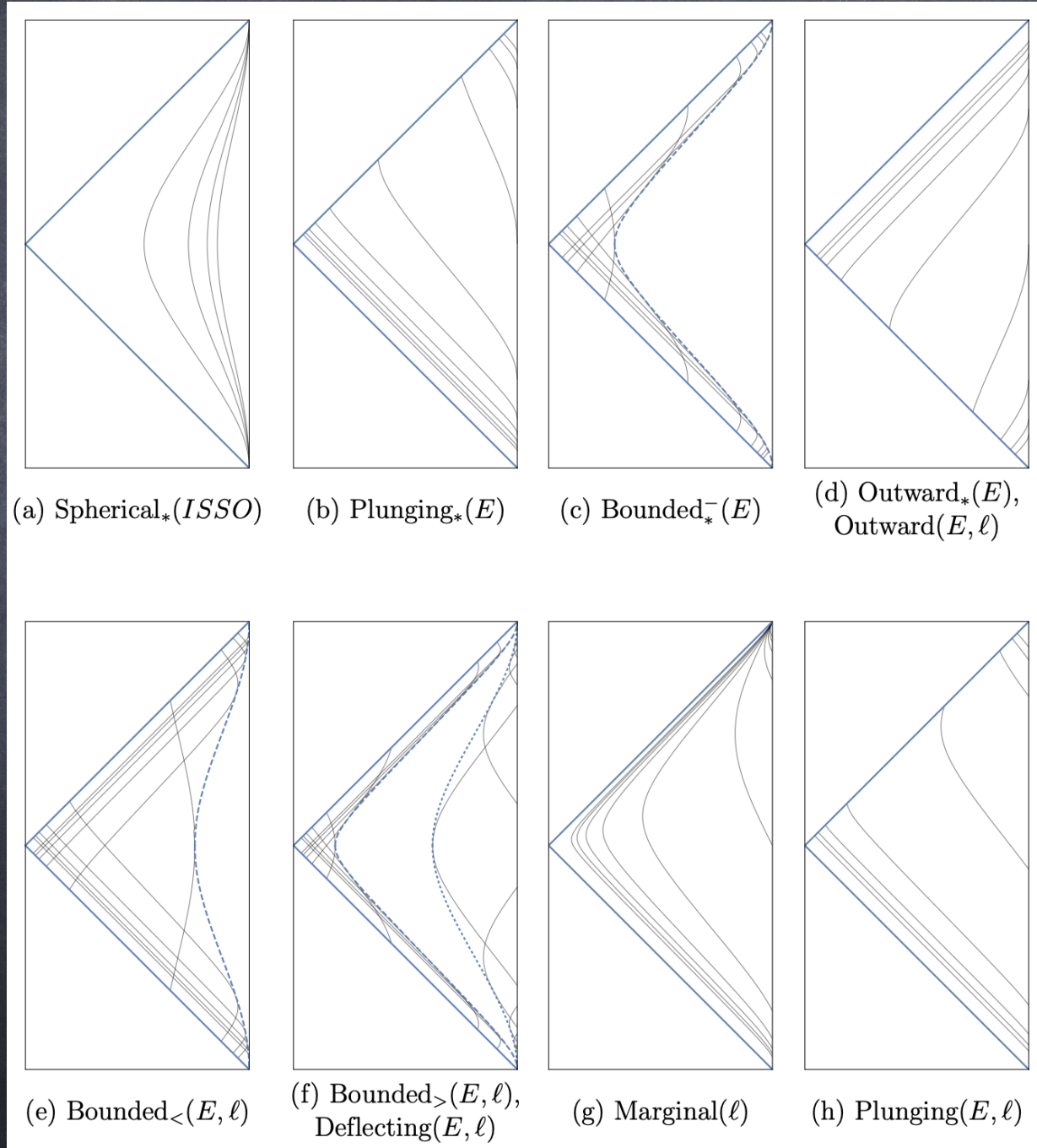


Matching region

Supercritical orbits

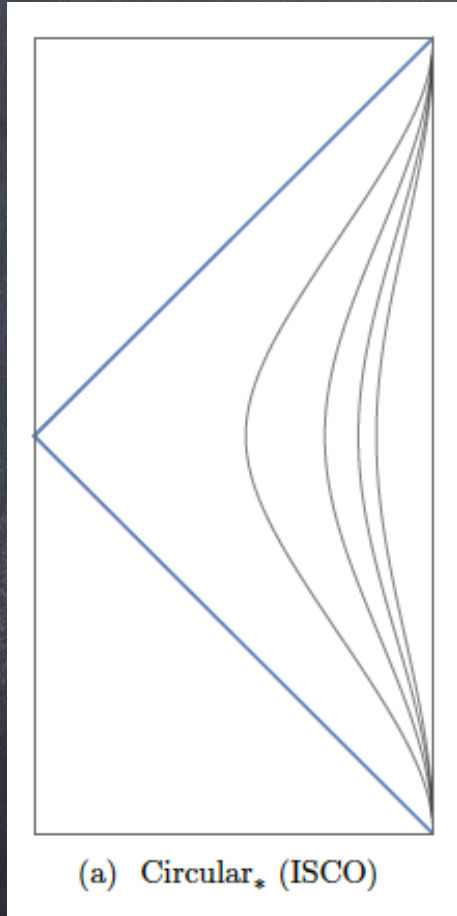
$$l > l_*$$

Geodesics can be classified (radially)



[Porfyriadis,
Strominger, 2014]
[Hadar, Porfyriadis,
Strominger, 2014]
[Kapec, Lupsasca,
2019]
[Compère, Druart,
2020]

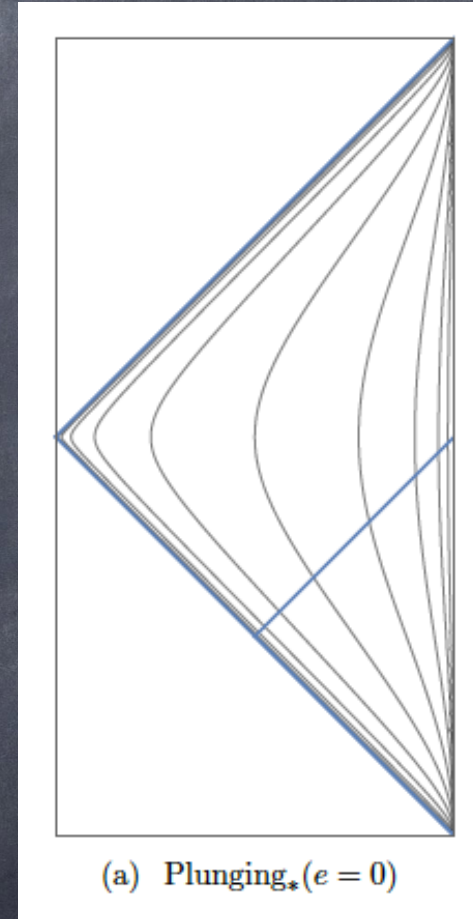
$SL(2, \mathbb{R})$ map of orbits



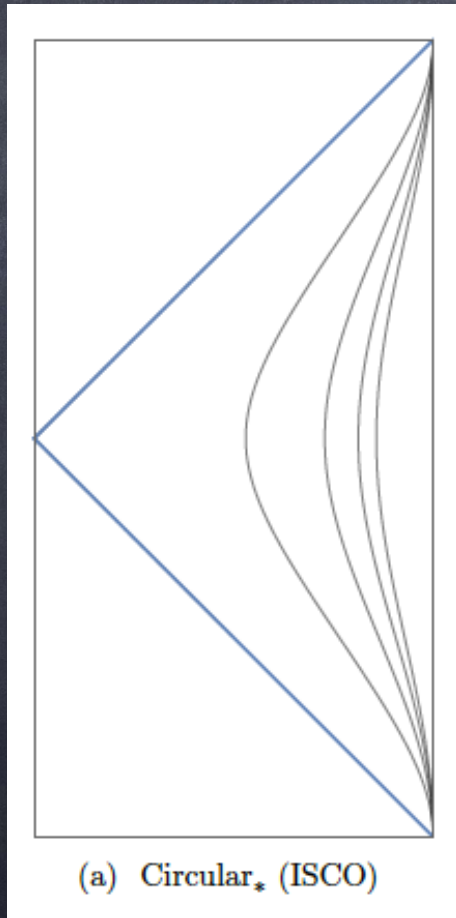
$SL(2, \mathbb{R})$ transformation



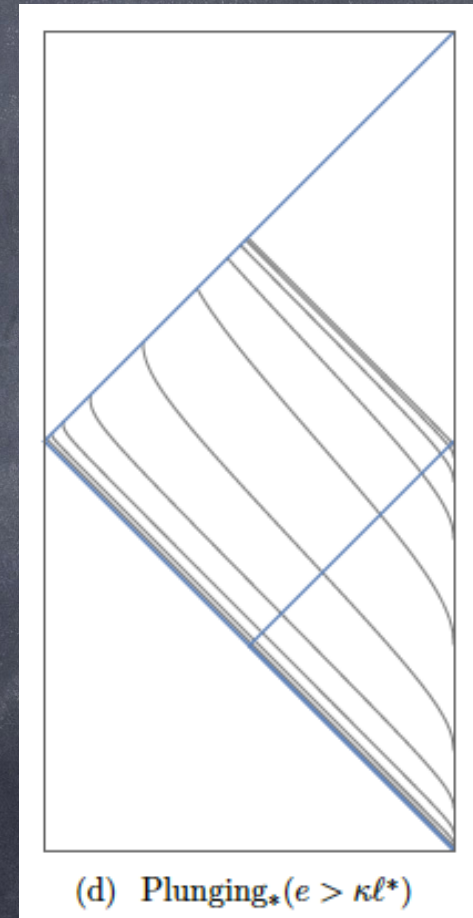
$$R = \frac{1}{\kappa} e^{\kappa t} \sqrt{r(r+2\kappa)},$$
$$T = -e^{-\kappa t} \frac{r+\kappa}{\sqrt{r(r+2\kappa)}},$$
$$\Phi = \phi - \frac{1}{2} \log \frac{r}{r+2\kappa}.$$



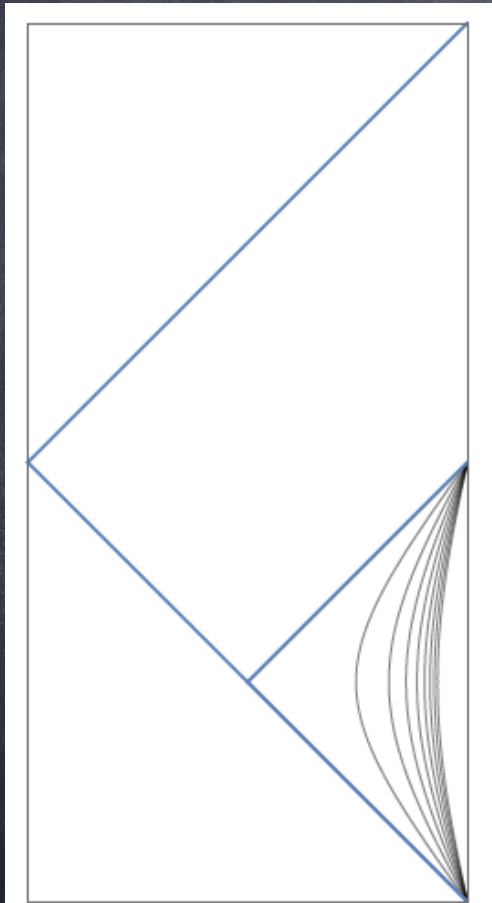
$SL(2, \mathbb{C}) \times U(1)$ map of orbits



$SL(2, \mathbb{C}) \times U(1)$
transformation



$SL(2, \mathbb{R}) \times PT$ map of orbits



(b)

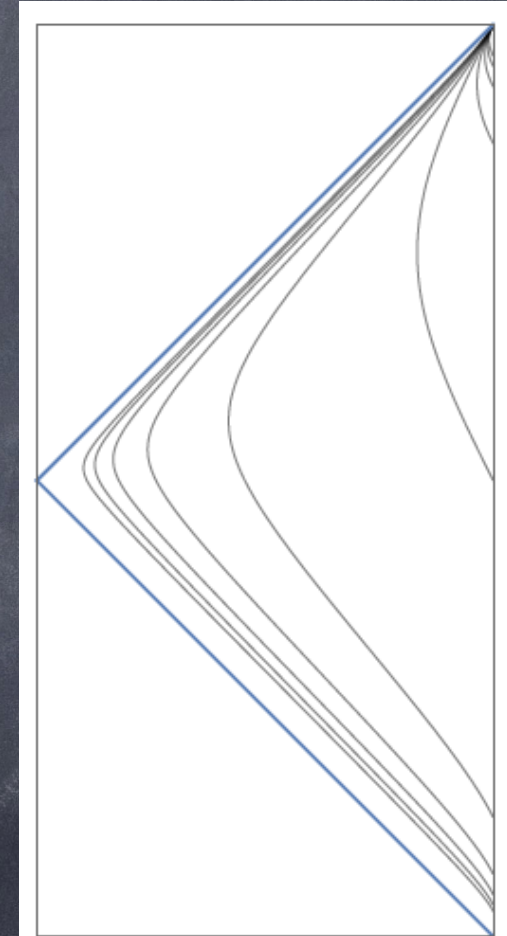
Circular(ℓ)

$SL(2, \mathbb{R}) \times PT$
transformation

$$\begin{aligned} r &= \kappa(-RT - 1), \\ t &= \frac{1}{\kappa} \log \frac{R}{\sqrt{R^2 T^2 - 1}}, \\ \phi &= \Phi + \frac{1}{2} \log \frac{-RT - 1}{-RT + 1}. \end{aligned}$$

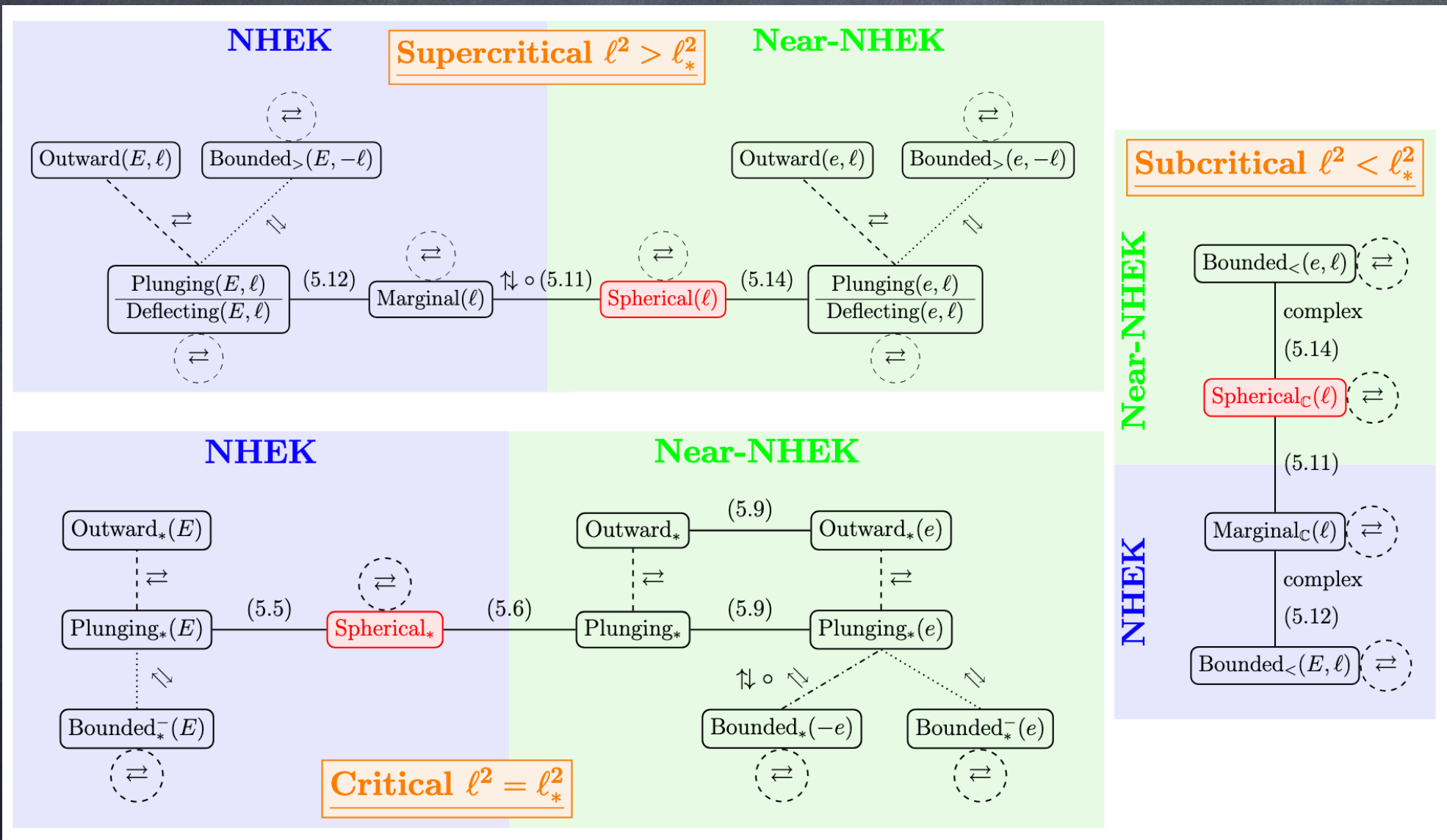
$$T \rightarrow -T$$

$$\Phi \rightarrow -\Phi$$

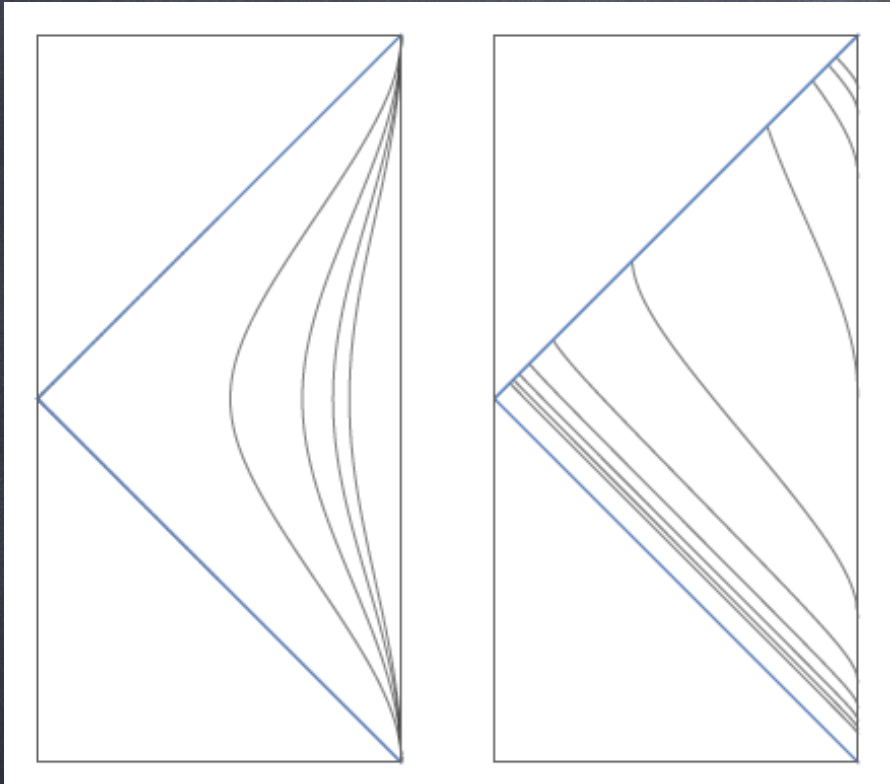


(d) Marginal(ℓ)

Geodesics are related by symmetry to (only!) 3 classes of spherical geodesics



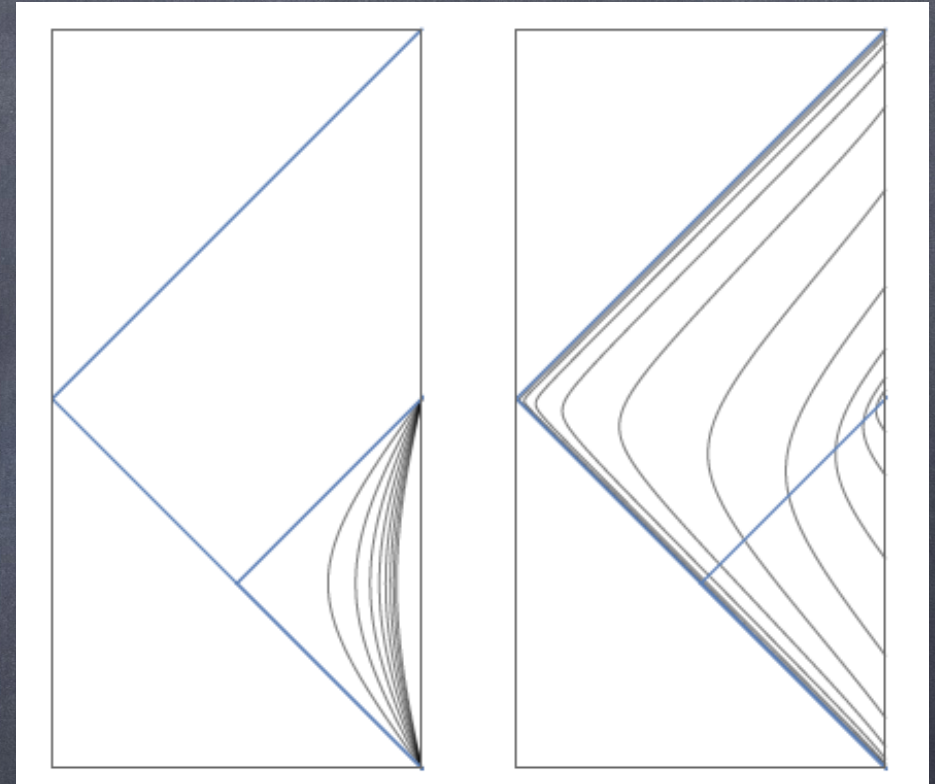
Feature #3: All incoming equatorial orbits belong to either of 2 conformal classes of orbits



Critical Conformal class

$$l = l_*$$

Contains circular NHEK orbit



Supercritical Conformal class

$$l > l_*$$

Contains circular near-NHEK orbit

[Compère, Fransen, Hertog, Long, 2018]

$SL(2, \mathbb{R}) \times U(1) \times (Z_2)^3$ symmetry leads to the "conformal method" to obtain analytic waveforms for plunges

- ① 1. Solve GW emission for circular orbits by brute force (Teukolsky method)
- ① 2. Apply symmetry transformations to obtain the GW waveforms for all geodesic plunges
- ① 3. Analytically resolve the conformal map of Dirichlet-Neumann boundary conditions (hypergeometric functions)
- ① 4. Analytically solve at late times in the QNM approximation (overtone sum over hypergeometric functions : results in polynomials and exponentials)

Feature #4: Bifurcation of Quasi-Normal Modes into: Zero damped (Near) and Damped modes (Far)

Zero damped QNM overtones have same real part of frequency and an equally spaced imaginary part

$$\hat{\omega}_{Nlm} = \frac{1}{2M}(m - i\lambda(N + h)) + o(\lambda)$$

Quasinormal modes (QNM)
of a Kerr black hole
for $l=2$ through 12
and first 8 overtones



This leads to Polynomial Quasi-normal Mode Ringing!

- Zero damped QNM overtones have same real part of frequency and an equally spaced imaginary part

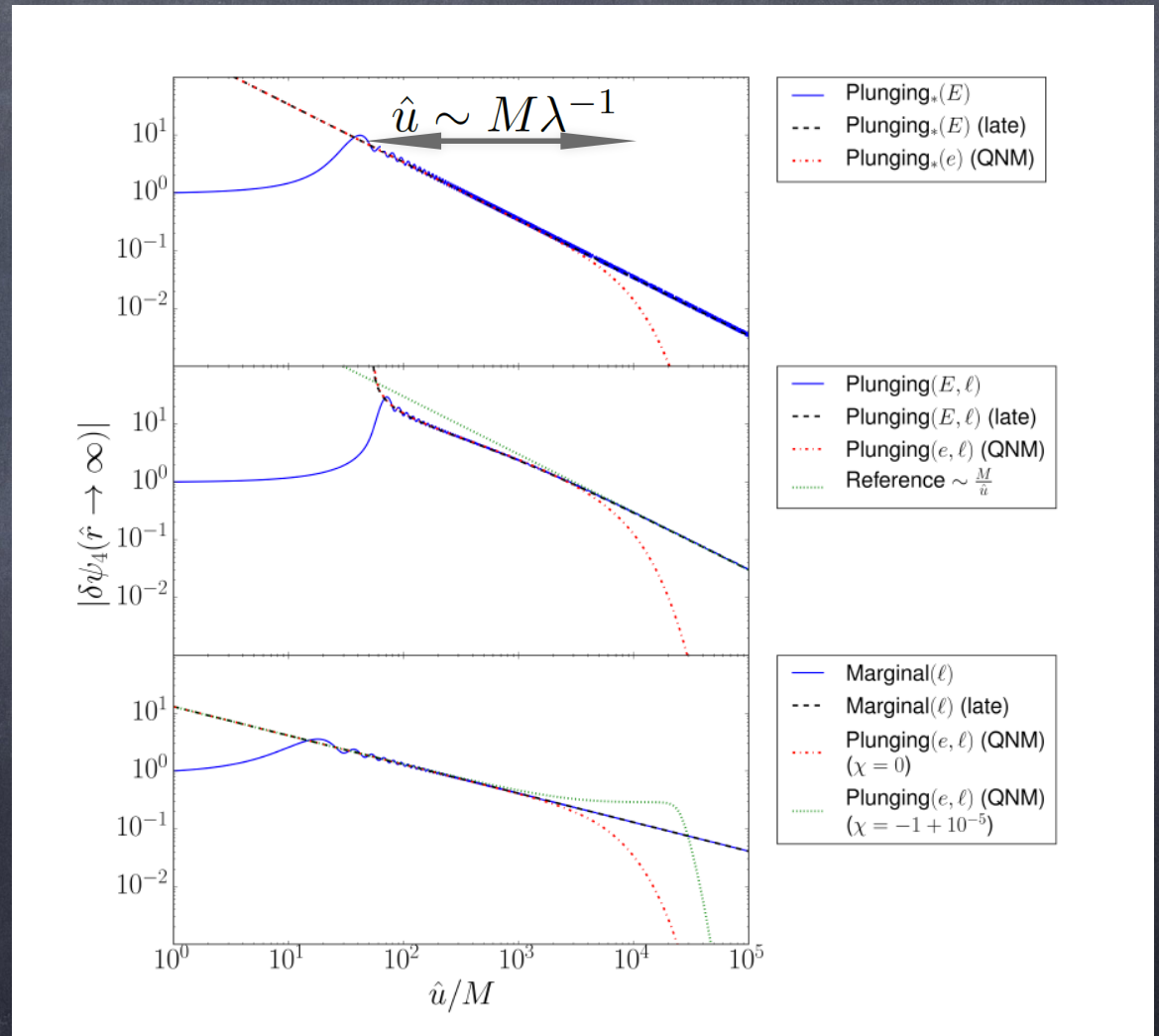
$$\hat{\omega}_{Nlm} = \frac{1}{2M}(m - i\lambda(N + h)) + o(\lambda)$$

- This might lead to a transient Polynomial Ringing due to coherent stacking of overtones

$$\sum_{N=0}^{\infty} e^{-N\lambda t} = \frac{1}{1 - e^{-\lambda t}} \approx \frac{1}{1 - (1 - \lambda t)} \approx \frac{1}{\lambda t} + O(\lambda t)$$

Smoking Gun #3: Polynomial Ringdown

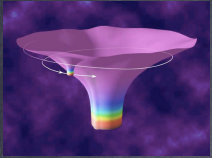
- GW Amplitude of plunges follows a late time power law continuously between $1/\sqrt{\hat{u}}$ and $1/\hat{u}$ before exponential decay
- The power analytically depends upon the impact parameters
- Time spent in polynomial ringdown :
 $\hat{u} \sim \lambda^{-1}$



[Compère, Fransen, Hertog, Long, 2018]

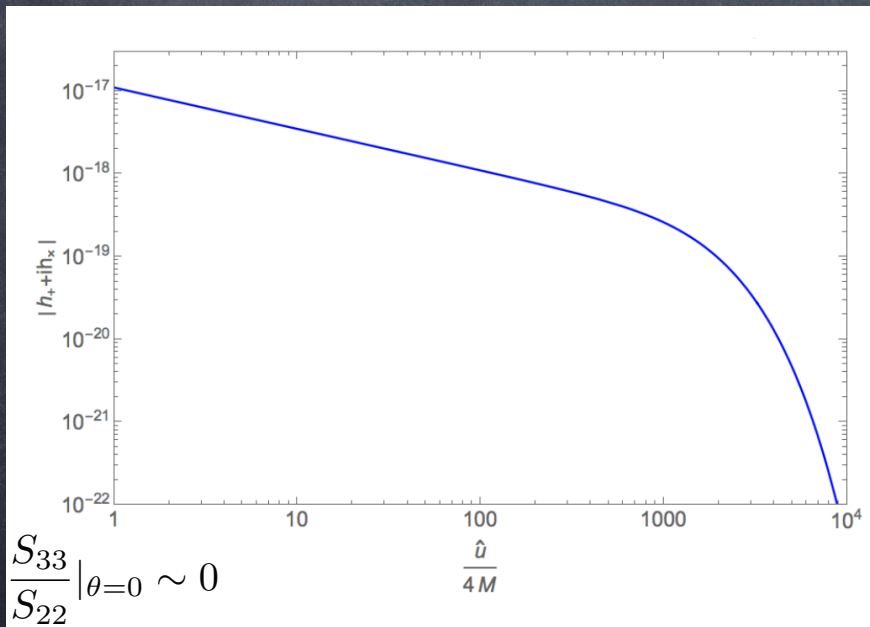
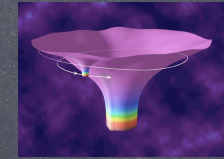
Smoking Gun #4

Emission of higher multipoles

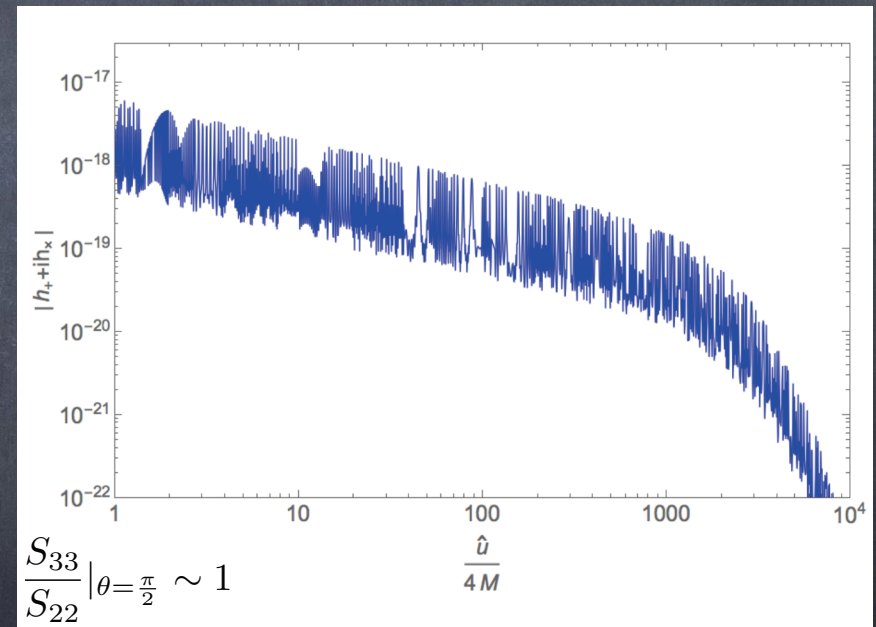


Face-On

Edge-On



$m = \ell = 2$ dominant

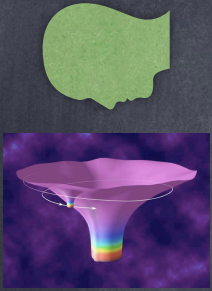


All m, ℓ up to 20 contribute

→ Enhanced sky localization of the source

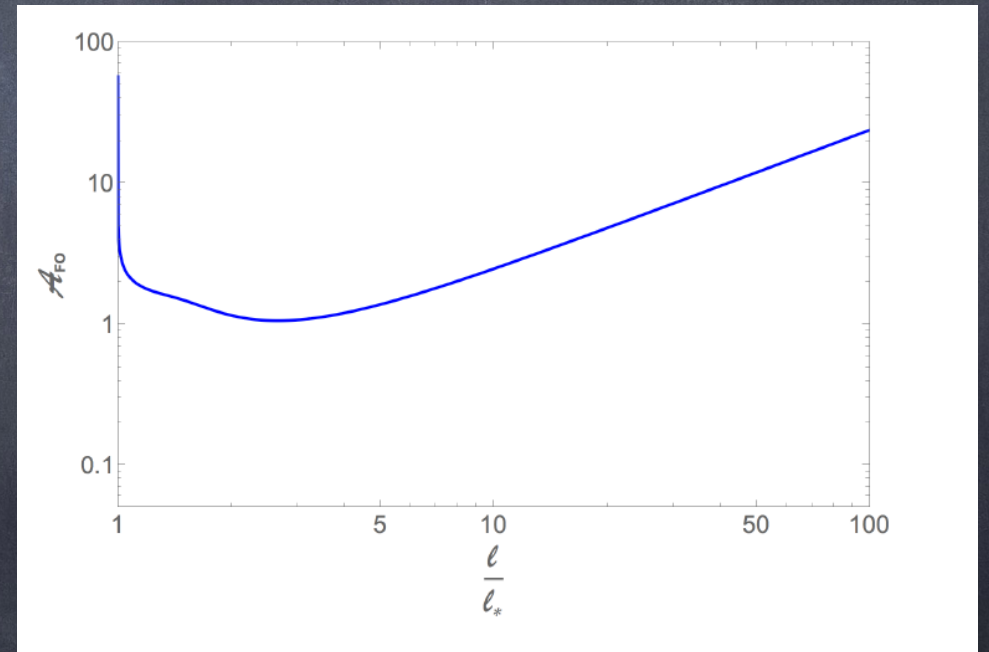
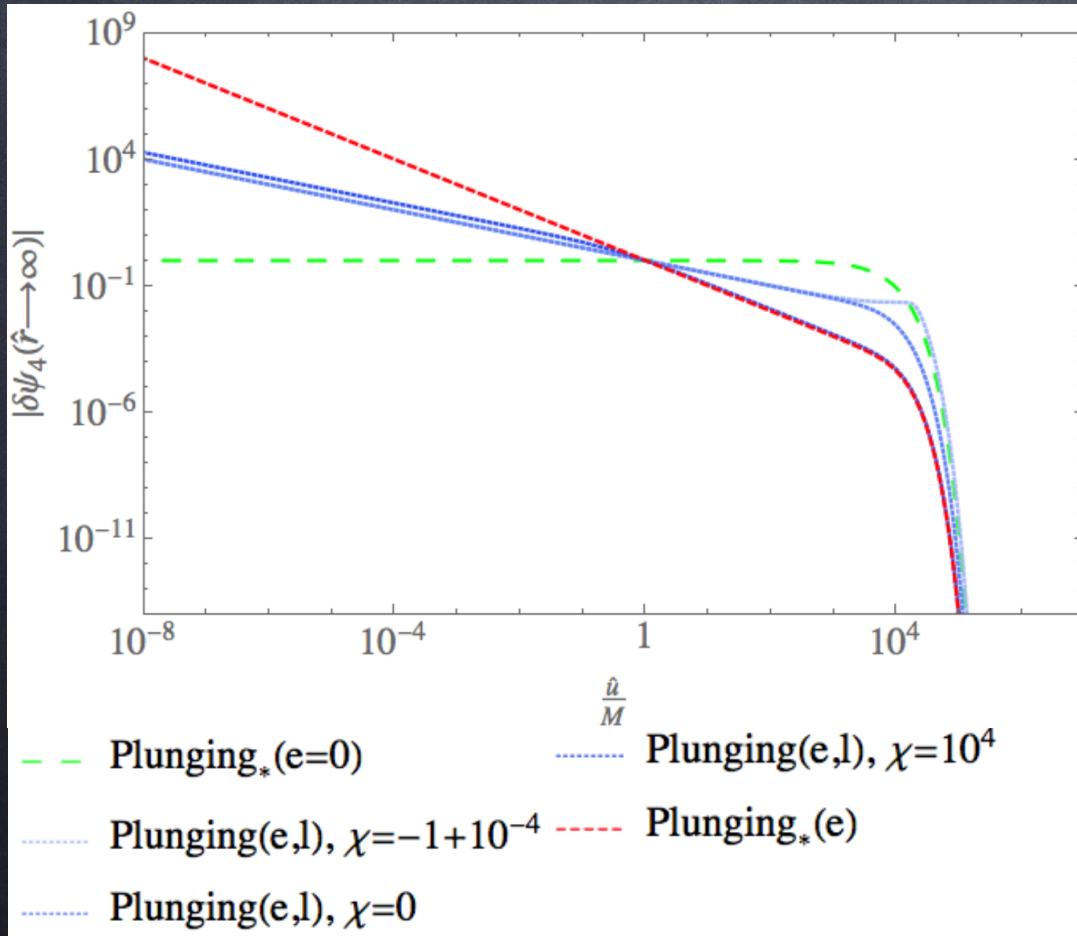
[Gralla, Hughes, Warburton, 2016] [Compère, Franssen, Hertog, Long, 2018]

Example: Face-on plunge



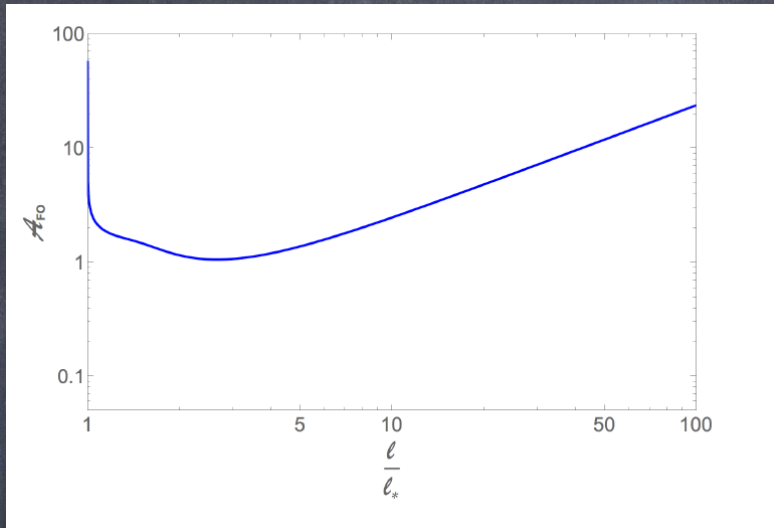
$$|h_+ + ih_\times| = \mathcal{A}_{FO} \left(\frac{\ell}{\ell_*} \right) \frac{m_0}{D} \frac{\sqrt{\lambda}}{(\sinh \frac{\lambda \hat{u}}{4M})^{1/2} (\cosh \frac{\lambda \hat{u}}{4M} + \chi \sinh \frac{\lambda \hat{u}}{4M})^{1/2}}$$

$$m = \ell = 2$$



[Compère, Franssen, Hertog, Long, 2018]

Feature #5: Critical behaviour

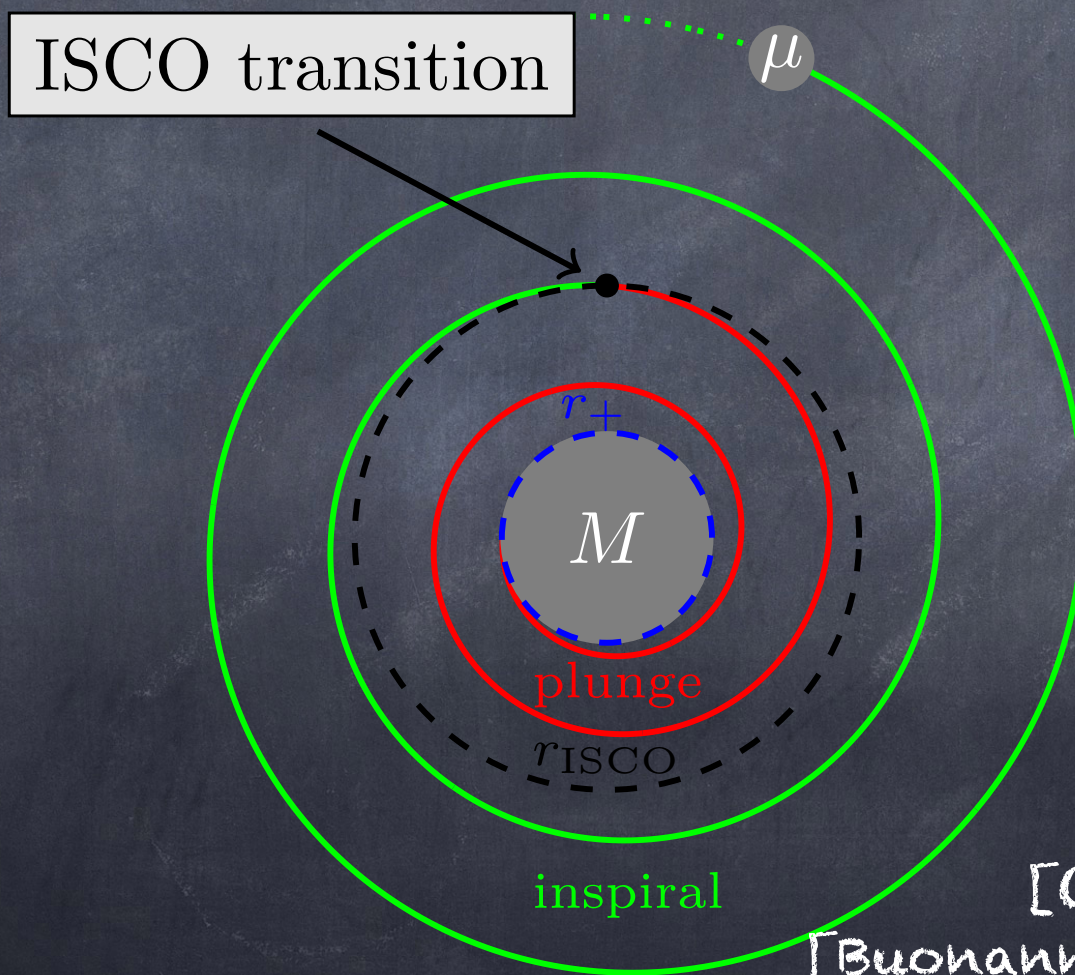


$$A_{FO}\left(\frac{l}{l_*} \rightarrow 1\right) = 1.1\left(\frac{l}{l_*} - 1\right)^{-\frac{1}{4}},$$
$$A_{FO}\left(\frac{l}{l_*} \rightarrow \infty\right) = 0.2\frac{l}{l_*}.$$

- Critical behaviour is a typical feature at near-extremality
- Divergence is capped by the match with the flat region:
This is the physics of a capped AdS₂.

$$A_{FO}\left(\frac{l}{l_*} \rightarrow 1\right) \sim \left(\frac{\lambda}{\sqrt{1 - \frac{l_*^2}{l^2}}}\right)^{1/2} \sim \sqrt{\frac{\hat{r}_{ISCO} - \hat{r}_+}{M}} \sim \lambda^{1/3}$$

Transition from Inspiral to Plunge



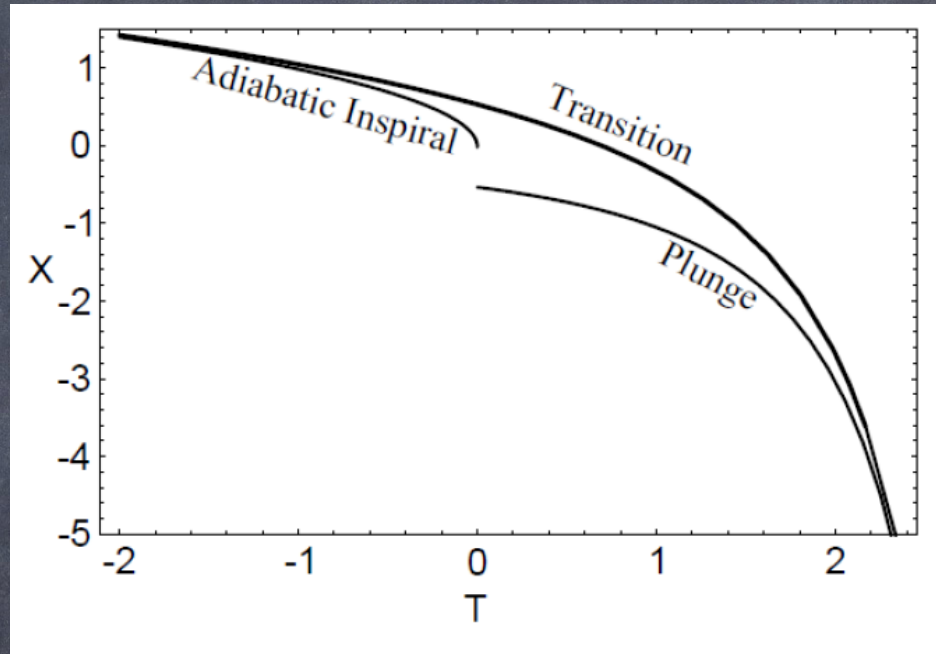
[Ori, Thorne, 2000]

[Buonanno, Damour, 2000]

[Kesden, 2011]

Transition from Inspiral to Plunge:

Standard Spin $\sqrt{1 - \frac{a^2}{M^2}} \ll \frac{\mu}{M}$



$$\frac{d^2 X}{dt^2} = -X^2 - t + O(\eta^{2/5}), \quad \frac{dY}{dt} = 2X + O(\eta^{2/5})$$

[Ori, Thorne, 2000]

[Kesden, 2011]

This is the Painlevé transcendent equation of the first kind.

The solution is not valid for Marginally/Extremely High Spins!

Transition from Inspiral to Plunge:

$$\text{High Spin } \sqrt{1 - \frac{a^2}{M^2}} \sim \frac{\mu}{M} \ll 1$$

The transition dynamics is now dictated by the equation

$$-\frac{2}{3}\psi - \frac{1}{3}\zeta \frac{d\psi}{d\zeta} + \psi \frac{d\psi}{d\zeta} + \omega^2 \frac{d^3\psi}{d\zeta^3} = 0.$$

$$t - t_* = \left(\frac{2}{9}\zeta + 2^{-2/3}\right) \left(\frac{\lambda}{\sigma_* \eta}\right)^{2/3},$$

$$R_N = \frac{2}{3}\psi(\zeta) - \frac{2}{3}\zeta,$$

$$\omega^2 = \frac{243}{4} \left(\frac{\sigma_* \eta}{\lambda}\right)^2,$$

This is the KdV equation with self-similar variables

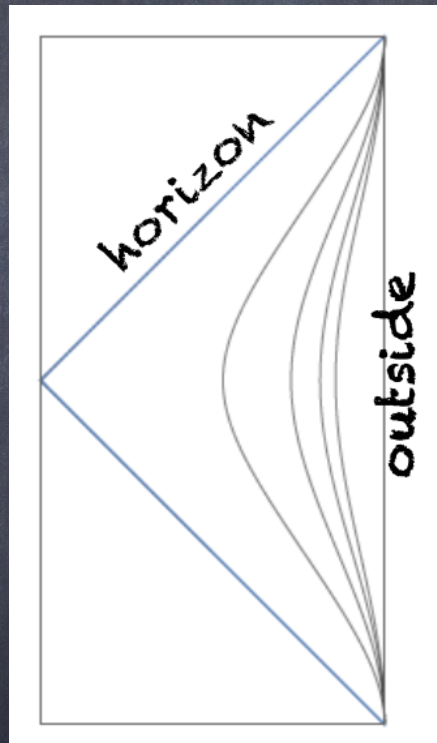
$$\frac{\partial \Psi}{\partial s} + \Psi \frac{\partial \Psi}{\partial z} + \omega^2 \frac{\partial^3 \Psi}{\partial z^3} = 0,$$

$$\zeta = \frac{z}{s^{1/3}}, \quad \psi(\zeta) = s^{2/3} \Psi(s, z).$$

The case $\sqrt{1 - \frac{a^2}{M^2}} \ll \frac{\mu}{M}$ is ruled out: the cross-section of angular momentum of the primary prevents it.

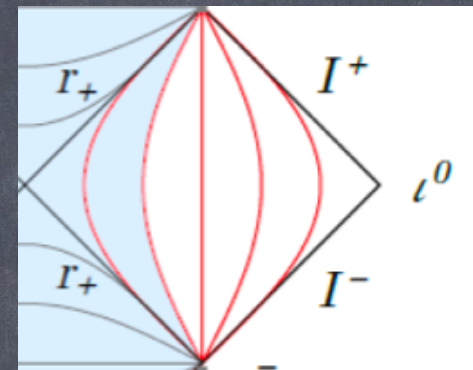
Feature #6: Non-decoupling between NHEK and the exterior region

NHEK



←
Travelling
waves
→

Exterior



"AdS₂ with finite cap"

[Amsel, Marolf, Horowitz, Roberts, 2009]

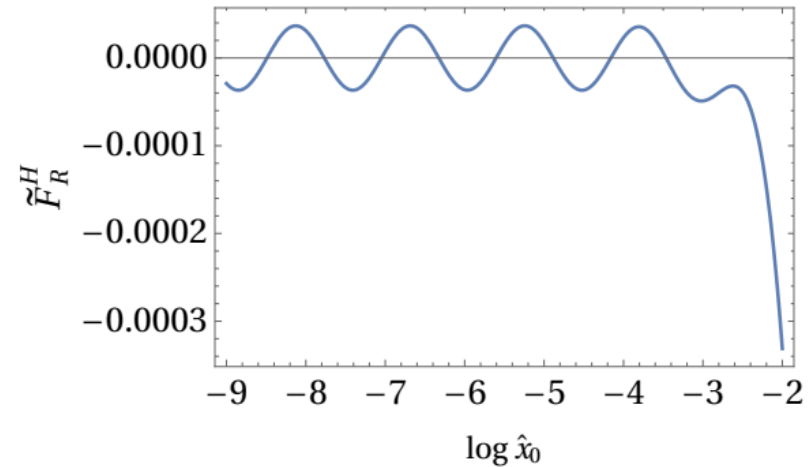
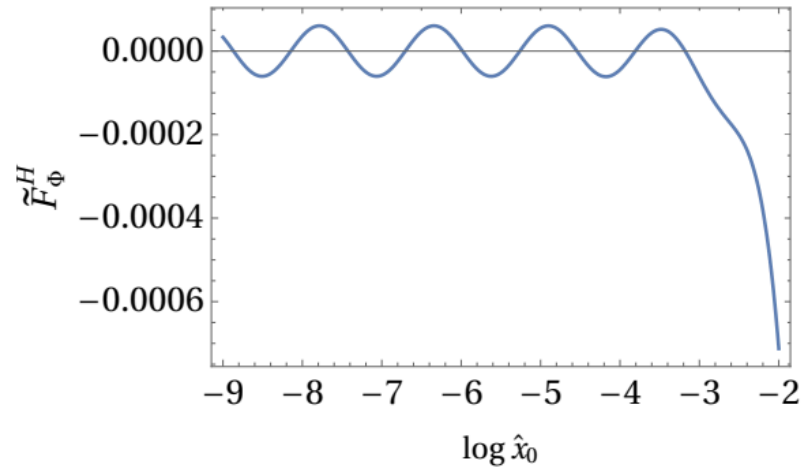
Neat example: scalar self-force

- Complex scalar in Kerr sourced by a point charge on a worldline

$$\nabla_\mu \nabla^\mu \Psi = -4\pi \rho, \quad \rho = q \int_\gamma \frac{\delta^{(4)}(x^\mu - z^\mu(\tau))}{\sqrt{-g}} d\tau.$$

- The self-force acting on the particle is $F_\mu(\tau) = \frac{q}{2} (\partial_\mu \Psi) |_{z(\tau)} + \text{c.c.}$
- We compute the self-force on a circular orbit in the NHEK geometry

Result



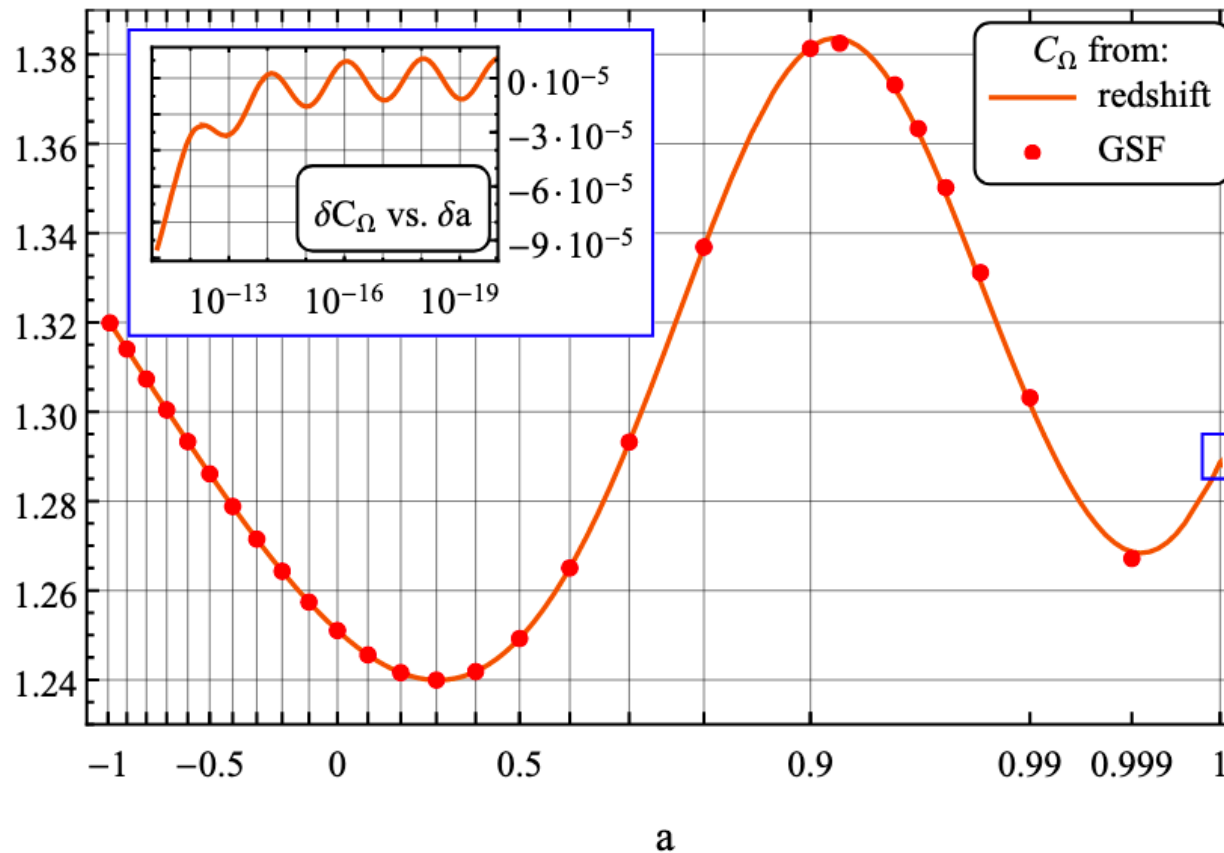
$$\hat{x}_0 \equiv \frac{\hat{r}_0 - \hat{r}_+}{M} = R_0 \lambda^{2/3}$$

The travelling wave $\ell = m = 2$ is dominant.

The self-force scales as $F_\mu \sim \cos(2\sqrt{-\eta_{22}} \log \hat{x}_0)$ where $h_{22} = \frac{1}{2}(1 + \sqrt{\eta_{22}})$ is the conformal weight corresponding to the $\ell = m = 2$ mode.

Conformal invariance is broken to discrete logarithmic periodicity

This effect is only seen in the extremely high spin limit



[van de Meent, 2016]

Conclusion

(Near-)extremal black holes

- 1) Make us think deeply about quantum gravity (effective field theory, singularities, quantum corrections, classical features, ...)
- 2) Have mysterious features (Kerr/CFT entropy match, zero entropy?, ...)
- 3) Lead to specific predictions for observation.
Caveat: very high spin is necessary, which is astrophysically very marginal!